CIDD: Collaborative Intelligence for Structure-Based Drug Design Empowered by LLMs

Bowen Gao[1,2]*, **Yanwen Huang**[3]*, **Yiqiao Liu**[3], **Wenxuan Xie**[4], **Bowei He**[5], **Haichuan Tan**[1], **Wei-Ying Ma**[1], **Ya-Qin Zhang**[1], **Yanyan Lan**[1,6,7]†

[1]Institute for AI Industry Research (AIR), Tsinghua University, Beijing, China
[2]Department of Computer Science and Technology, Tsinghua University, Beijing, China
[3]Department of Pharmaceutical Science, Peking University, Beijing, China
[4]School of Future Technology, South China University of Technology, Guangzhou, China
[5]Department of Computer Science, City University of Hong Kong, Hong Kong SAR, China
[6]Beijing Frontier Research Center for Biological Structure, Tsinghua University, Beijing, China
[7]Beijing Academy of Artificial Intelligence (BAAI), Beijing, China

Abstract

Structure-guided molecular generation is pivotal in early-stage drug discovery, enabling the design of compounds tailored to specific protein targets. However, despite recent advances in 3D generative modeling, particularly in improving docking scores, these methods often produce uncommon and intrinsically unreasonable molecular structures that deviate from drug-like chemical space. To quantify this issue, we propose a novel metric, the Molecule Reasonable Ratio (MRR), which measures structural rationality and reveals a critical gap between existing models and real-world approved drugs. To address this, we introduce the Collaborative Intelligence Drug Design (CIDD) framework, the first approach to unify the 3D interaction modeling capabilities of generative models with the general knowledge and reasoning power of large language models (LLMs). By leveraging LLM-based Chain-of-Thought reasoning, CIDD generates molecules that are not only compatible with protein pockets but also exhibit favorable drug-likeness, structural rationality, and synthetic accessibility. On the CrossDocked2020 benchmark, CIDD consistently improves drug-likeness metrics, including QED, SA, and MRR, across different base generative models, while maintaining competitive binding affinity. Notably, it raises the combined success rate (balancing drug-likeness and binding) from 15.72% to 34.59%, more than doubling previous results. These findings demonstrate the value of integrating knowledge reasoning with geometric generation to advance AI-driven drug design.[3]

1 Introduction

Structure-based drug design (SBDD) enables the direct generation of compounds tailored to protein binding sites, making it a powerful tool in drug discovery. Recent 3D generative models—including autoregressive approaches like AR [24] and Pocket2Mol [25], and diffusion-based methods such as TargetDiff [12], DecompDiff [13], and MolCRAFT [26]—have advanced rational molecule design. However, expert evaluation often reveals chemically unreasonable features, such as overly fused polycyclic systems and partially unsaturated rings (Figure 1a). While these distortions may improve

[*] Equal contribution

[†] Correspondence to lanyanyan@air.tsinghua.edu.cn

[3] Code is available at https://github.com/bowen-gao/CIDD/.

39th Conference on Neural Information Processing Systems (NeurIPS 2025).

docking scores via geometric complementarity, they often compromise intramolecular stability and result in poor pharmacokinetic properties.

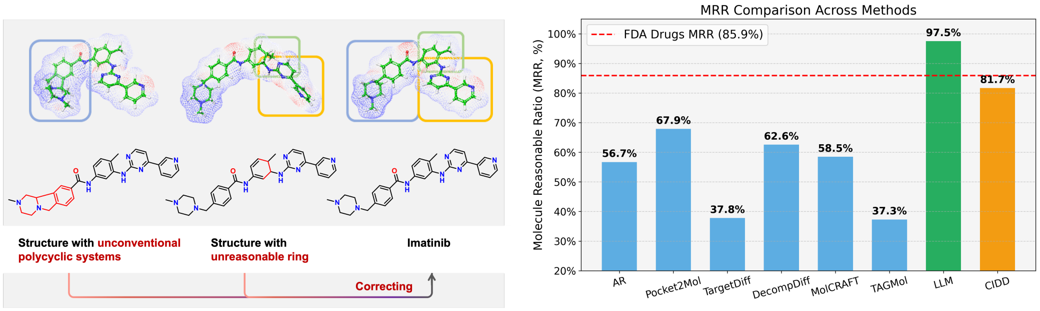

(a)

(b)

Figure 1: (a) **Common errors in 3D-SBDD outputs.** Minor structural changes can cause large deviations in 3D conformation, highlighting the challenge of correcting chemically uncommon structures without disrupting valid 3D shapes. (b) **MRR comparison.** While FDA drugs reach 85.9% MRR, existing 3D models lag behind. LLM achieves 97.5%, and CIDD closes the gap with 81.7%.

While current models effectively generate molecules that fit target pockets, they often overlook the physicochemical and pharmacological features common to clinically approved drugs. These limitations stem from a fundamental mismatch: the narrow focus on binding-site compatibility often comes at the expense of structural reasonability and drug-likeness, which depend solely on the chemical structure itself and often conflict with geometric fit. To quantify the gap, we propose the **Molecular Reasonability Ratio (MRR)**, which measures the proportion of generated molecules that are structurally valid and chemically reasonable relative to drug-like standards. As shown in Figure 1b, based on our experiments, existing 3D generative models perform poorly under this metric (e.g., TargetDiff: 37.8%, MolCRAFT: 58.5%), falling well below the 85.9% observed in FDA-approved drugs. Some recent methods, such as TAGMol, build on TargetDiff by incorporating gradient-based guidance to jointly optimize for drug-likeness properties like QED [3]. While this leads to improvements in QED scores, it does not result in a general enhancement of drug potential, as evidenced by TAGMol's similarly low MRR. In contrast, LLMs achieve high MRRs on SBDD tasks (e.g., GPT-4: 97.5%) thanks to their general chemical and pharmaceutical knowledge, but they struggle to generate molecules with high binding affinity due to limited spatial reasoning and the inherent trade-off between potency and drug-likeness.

To bridge this gap, we propose **CIDD**—a **Collaborative Intelligence for Drug Design** framework that combines the interaction modeling capabilities of 3D generative models with the domain knowledge and instruction following strengths of LLMs. Rather than directly producing final drug candidates, 3D models generate interaction-focused molecular proposals that capture key binding features. These serve as structured input for an LLM-driven design process that translates spatial intent into chemically viable drug-like molecules. This division of roles allows CIDD to generate compounds that are both interaction-competent and structurally plausible. CIDD decomposes the generation task into a series of specialized modules, each powered by the LLM. The *Interaction Analysis Module* identifies fragment-level interactions; the *Design Module* proposes chemically informed modifications; the *Reflection Module* provides analysis; and the *Selection Module* ranks candidates by interaction quality and chemical coherence. CIDD follows a structured **Chain-of-Thought (CoT)** prompting strategy guided by domain knowledge guided prompts, enabling interpretable, stepwise molecular design. **This modular, CoT-guided architecture mirrors real-world medicinal chemistry workflows and enables the generation of pharmaceutically relevant, structurally sound compounds.**

Evaluated on the CrossDocked2020 dataset [9], CIDD significantly outperforms state-of-the-art baselines, boosting the overall success ratio from **15.72% to 34.59%**. It consistently improves key drug-likeness metrics—including *Quantitative Estimation of Drug-likeness* (QED) [3], synthetic accessibility (SA), MRR, and the proportion of molecules meeting QikProp [30] thresholds—across diverse baseline models. **Our key contributions are:**

(1) **Identifying a core limitation in current SBDD models:** We introduce the **MRR** to assess intrinsic structural rationality, revealing that pocket-based 3D generative models often produce

intrinsically irrational and rare molecules that deviate from drug-like chemical space despite favorable docking scores.

(2) **A unified framework for rational molecule generation:** We propose **CIDD**, the first framework to combine the spatial modeling of 3D generative models with the chemical reasoning capabilities of LLMs. By leveraging their complementary strengths, CIDD uses Chain-of-Thought guidance to overcome the common trade-off between binding affinity and drug-likeness.

(3) **Validated performance and broader implications:** CIDD achieves state-of-the-art results on CrossDocked2020, significantly improving drug-likeness metrics (QED, SA, MRR) while preserving binding affinity. This demonstrates its effectiveness and highlights the advantage of combining LLMs with geometric modeling for AI-driven drug design.

2 Preliminaries

2.1 Structure-Based Drug Design

The goal of SBDD is to generate a molecule x that binds to a given protein pocket P. Recent work has explored a variety of deep generative approaches. LiGAN [27] uses a conditional variational autoencoder (CVAE) to generate 3D point clouds of ligands conditioned on pocket geometry. Autoregressive models such as AR [24] and Pocket2Mol [25] sequentially construct molecules in 3D space. Diffusion-based methods like TargetDiff [12], IPDiff [15], and DecompDiff [13] iteratively refine 3D structures or molecular graphs, while TAGMol [7] further applies gradient-based optimization during generation. Other approaches include the fragment-based DrugGPS [37] and MolCRAFT [26], a Bayesian flow model that learns the distribution of drug-like molecules conditioned on pocket structures. All these methods generate intermediate 3D point clouds or graphs, which are subsequently mapped into chemically valid molecules as the final output.

2.2 Large Language Models

LLMs are advanced neural networks trained on vast corpora of textual data, enabling them to understand, generate, and reason with human-like language. Notable examples include GPT-4 [2], LLaMA [33], ChatGLM [11], and DeepSeek [21], which have demonstrated impressive capabilities in tasks such as natural language understanding, code generation, mathematical problem solving, and logical reasoning. Their versatility and ability to capture complex patterns have made them increasingly relevant in domains beyond traditional natural language processing, including drug discovery [4]. Recent work has explored the use of LLMs to generate or modify molecules with desired properties. For example, ChatDrug [22] employs conversational LLMs for generating and editing molecules with desired properties. However, the application of LLMs to *pocket-based* molecular design remains largely unexplored. This is primarily due to the challenge of capturing essential three-dimensional structural information, which is critical for modeling protein-ligand interactions. Unlike textual or sequence-based data, protein binding pockets and small molecules interact through spatially complex, non-linear, and chemically rich environments that cannot be directly encoded in natural language.

3 Methods

3.1 Evaluating the Gap Between Generated Molecules and Real Drugs

Drug-likeness is an inherently multidimensional attribute that dictates the probability $p(\text{drug})$ that a molecule will reach its biological target—an assessment that precedes, and is distinct from, estimating binding affinity. Widely used machine-learning surrogates, most notably QED [3] and Lipinski's Rule of Five [20], are inadequate for two principal reasons: (i) Legacy bias: These metrics were calibrated on historical chemical space and fail to recognize the unconventional scaffolds produced by modern generative models. Consequently, structurally implausible or pharmacologically irrelevant molecules can still achieve high "drug-like" scores. (ii) Oversimplification: QED relies on only seven physicochemical descriptors, and its average value for DrugBank [17] molecules is below 0.5, illustrating its limited discriminative power.

To close this gap, we introduce a broader evaluation framework comprising two complementary tiers. Structural reasonability screens for fundamental medicinal-chemistry principles such as aromaticity, ring-system stability, and hybridization consistency, while physicochemical and pharmacokinetic suitability evaluates absorption, distribution, metabolism, excretion, and toxicity (ADME/T) properties using established descriptors. Together, these tiers ensure that generated molecules are both chemically plausible and therapeutically relevant, providing a more reliable benchmark for modern AI-driven molecular design.

Molecular Reasonability Ratio. To address the lack of metrics capable of identifying the structural gap between generated molecules and rationally designed drugs, we introduce MRR as a targeted solution. MRR is a rule-based, empirically motivated metric designed to flag structures that are uncommon in medicinal chemistry practice. Its design is informed by expert analyses of SBDD outputs, which consistently reveal a predominant failure mode: the improper use of ring conjugation—particularly aromaticity—that often deviates from patterns observed in clinically validated drugs.

MRR operates by analyzing the hybridization states of atoms within a molecule. It sequentially excludes fully aromatic or fully saturated rings and focuses on the remaining atoms within each ring system. After removing peripheral substituents, if the hybridization states of the residual ring atoms are neither all sp^2 nor all sp^3, the structure is classified as chemically unreasonable. For example, structures such as cyclohexene and cyclohexa-1,3-diene are flagged, as they likely result from the model's failure to correctly generate either fully aromatic or fully saturated systems. Although not intended as an exhaustive classifier, MRR provides an interpretable, medicinal-chemistry-guided screen that complements basic valence checks and ADME filters, thereby reducing the incidence of structurally implausible candidates generated by models. The full algorithm for MRR is shown in Appendix D.

QikProp Multiple Property Requirements. To further evaluate the physicochemical and pharmacokinetic properties of the generated molecules, we employ QikProp [30], a tool recognized for its robust performance in predicting molecular drug-likeness properties [16]. The assessed properties include aqueous solubility, lipophilicity, polar surface area (PSA), the number of metabolizable sites, and oral absorption. Detailed requirements for each property are provided in Appendix E.

A molecule is considered to have passed the evaluation if it satisfies all N predefined property requirements: $P_1, P_2, \ldots, P_N$. If any of the properties fall outside the acceptable range, the molecule is classified as failing.

$$\text{QikProp} = \begin{cases} 1 & \text{if } P_1 \land P_2 \land \cdots \land P_N \text{ are satisfied,} \\ 0 & \text{otherwise.} \end{cases}$$

3.2 Bridging the Gap with CIDD framework

We propose the **Collaborative Intelligence Drug Design (CIDD)** framework (Figure 2), a modular system for target-specific molecule generation that combines 3D interaction modeling with LLM-enhanced molecular design. It consists of two components: the **Structure-Based Interaction Generator (SBIG)** and the **LLM-Enhanced Drug Designer (LEDD)**.

SBIG uses 3D generative models to produce *interaction-oriented molecular structures*—intermediates that fit the protein pocket but might be chemically incomplete.

LEDD then refines these raw proposals into drug-like molecules using LLMs. The whole process is formalized as:

$$x_0 = \texttt{SBIG}(\textit{Target}), \quad x = \texttt{LEDD}(x_0, \textit{Target})$$

Here, x_0 encodes the intended spatial interactions, and LEDD completes it into a chemically valid, synthetically accessible compound x. A key limitation of prior approaches is the absence of ground-truth mappings from interaction scaffolds to drug-like molecules, making supervised training infeasible. Traditional generative models—based on direct optimization or limited heuristics—struggle to bridge this gap. In contrast, LEDD leverages the implicit drug-relevant knowledge embedded in large-scale pretrained LLMs. With strong **instruction-following, reasoning, and coordination abilities**,

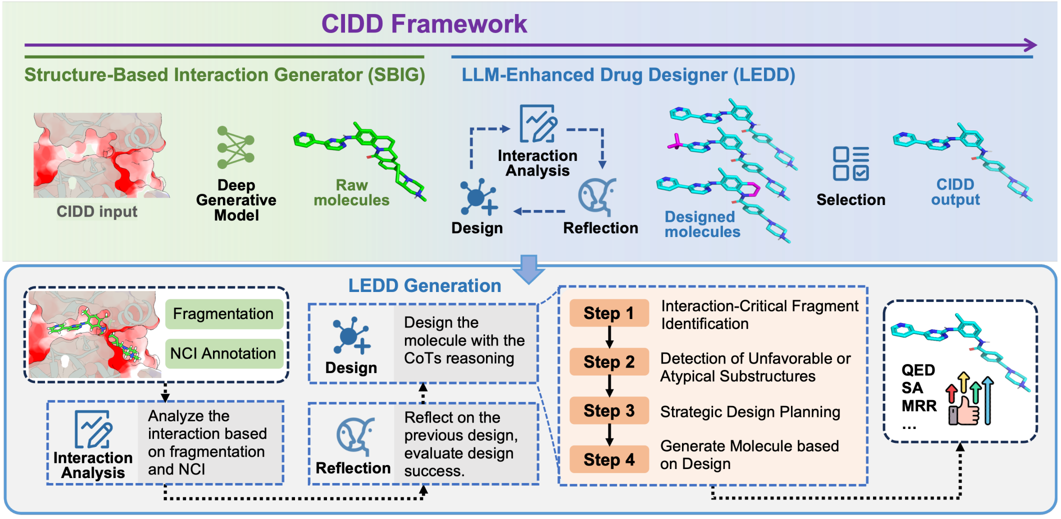
CIDD Framework
Structure-Based Interaction Generator (SBIG)
LLM-Enhanced Drug Designer (LEDD)
CIDD input
Deep Generative Model
Raw molecules
Interaction Analysis
Design
Reflection
Designed molecules
Selection
CIDD output
LEDD Generation
Fragmentation
NCI Annotation
Design
Design the molecule with the CoTs reasoning
Interaction Analysis
Analyze the interaction based on fragmentation and NCI
Reflection
Reflect on the previous design, evaluate design success.
Step 1
Interaction-Critical Fragment Identification
Step 2
Detection of Unfavorable or Atypical Substructures
Step 3
Strategic Design Planning
Step 4
Generate Molecule based on Design
QED
SA
MRR
...

Figure 2: **Overview of the CIDD framework.** Top: end-to-end pipeline integrating SBIG and LEDD. Bottom: detailed view of LEDD's LLM-based design process, which designs and generates molecules through interaction analysis, reflection, and Chain-of-Thought-driven reasoning.

the LLM enables design decisions that generate molecules without incurring the typical trade-offs between potency and drug-likeness in drug design.

The CIDD framework is inspired by the real-world workflow of medicinal chemists, who begin by identifying key interaction patterns between a ligand and its target, and then construct molecules that retain these interactions while satisfying broader drug development constraints. CIDD formalizes this reasoning process: SBIG captures spatial interaction intent, while LEDD—powered by LLMs—assumes the role of a virtual chemist to transform raw scaffolds into viable drug-like molecules. By leveraging the LLM's instruction-following and general knowledge, CIDD effectively substitutes human expertise in the molecule design process.

3.2.1 Pipeline Overview

CIDD decomposes the complex task of drug-oriented molecule generation into a structured pipeline of modular reasoning steps. It begins with SBIG, which generates interaction-focused intermediate structures conditioned on the target pocket. These intermediates are passed to the **Interaction Analysis Module**, which extracts fragment-level binding profiles using docking, fragmentation, and rule-based NCI detection. The **Design Module** then interprets these profiles to generate chemically plausible molecules that maintain critical interaction motifs. Each design is re-evaluated, and its updated interaction profile is processed by the **Reflection Module**, which compares successive design states and produces feedback for new designs. After generating N new candidates, the **Selection Module** ranks all candidates based on their interaction quality and chemical viability, selecting the final molecule for downstream use. This modular pipeline mirrors expert workflows and enables interpretable, multi-stage control over both structural interaction and chemical relevance.

3.2.2 Interaction Analysis Module

This module evaluates the molecular interaction between a candidate molecule x_i and a target protein pocket P. The process begins by re-docking x_i into the binding site of P to generate a protein–ligand complex conformation. The molecule x_i is then decomposed into chemically meaningful fragments via the BRICS algorithm [6], enabling fragment-level attribution of interaction features.

Next, non-covalent interactions (NCIs), such as hydrogen bonding, π–π stacking, salt bridges, and hydrophobic contacts, are identified from the docked complex based on geometric and chemical features. The resulting interaction map—capturing both atomic contacts and fragment-level organization—is then analyzed by an interaction-specialized large language model, LLM_I. Conditioned on spatial interaction cues and chemical context, LLM_I synthesizes this information into a structured interaction profile I_i, which semantically links molecular fragments to their respective roles in target engagement.

Formally, the process can be represented as:

$$\mathrm{LLM}_I(x_i, P) \to I_i$$

The resulting profile I_i provides fragment-level interpretation of binding contributions and serves as the basis for chemically informed design in subsequent modules.

3.2.3 Design Module

Given a raw molecule x_0, its interaction report I_0, and prior feedback from the reflection module $R = \{R_1, R_2, \ldots, R_{i-1}\}$, the Design Module leverages an LLM with a Design role (LLM_D) to produce a refinement plan D_i and an updated molecule x_i.

$$LLM_D(x_0, I_0, R) \to (D_i, x_i)$$

Here, D_i is a structured and interpretable set of design decisions grounded in medicinal chemistry, and x_i is the generated compound for further evaluation.

To emulate real-world drug design workflows, we implement a **Chain-of-Thought** prompting strategy that guides the LLM through a domain-informed reasoning pipeline with four sequential stages. **(1) Interaction-Critical Fragment Identification:** the model analyzes x_0 and highlights fragments forming key non-covalent interactions with the target, based on I_0. **(2) Detection of Unfavorable or Atypical Substructures:** chemically undesirable fragments—such as synthetically inaccessible motifs, strained rings, or poor physicochemical regions—are flagged for replacement. **(3) Strategic Design Planning:** the model proposes modifications that improve chemical viability while preserving interaction and topology, often substituting problematic regions with pharmaceutically preferred alternatives. **(4) Candidate Molecule Generation:** a new structure x_i is generated based on the design plan, ensuring both target interaction and drug-like properties.

By encoding expert priors into the prompt structure, the Design Module reframes molecule generation as a chemically grounded reasoning task. The LLM is able to coordinate multiple design objectives within a unified framework. This enables the CIDD to effectively mitigate the trade-offs between affinity and drug-likeness that commonly arise in drug design. It bridges raw interaction scaffolds to viable candidate molecules in a transparent and interpretable manner.

3.2.4 Reflection and Selection Modules

The *Reflection Module* evaluates whether each candidate design x_i achieves design goals by comparing it to the initial raw molecule x_0 and their respective interaction profiles:

$$LLM_R(x_0, I_0, D_i, x_i, I_i) \to R_i$$

The *Selection Module* evaluate all the designed molecules $\{x_1, x_2, \ldots, x_N\}$ and their interaction reports to identify the most promising candidate:

$$LLM_S\left(\{(x_1, I_1), \ldots, (x_N, I_N)\}\right) \to x_{\text{best}}$$

Here, x_{best} balances interaction quality and chemical viability. Full prompt examples for each module are in Appendix C.

4 Experiments

4.1 Experiment Settings

Dataset. We follow prior 3D-SBDD settings and use the CrossDocked2020 dataset [9], adopting the same train/test split as TargetDiff [12], resulting in 100 protein pockets for test.

Metrics. We evaluate models using standard metrics: Vina docking score [34] for binding affinity, QED [3] for drug-likeness, SA score [8] for synthetic accessibility, and molecular diversity (computed as 1 − ECFP4 similarity [29]) for structural variety. As we do not directly generate 3D conformations, Vina Score/Min is excluded. Beyond conventional metrics, we emphasize the evaluation of **drug potential** via two additional metrics: **MRR (Molecular Rule-based Reasonability)**, which captures domain-informed structural plausibility, and **QikProp pass ratio**, which assesses a wide range of physicochemical and pharmacokinetic properties. Together with QED and SA, these offer a more holistic assessment of molecular viability. We also report the success ratio, defined as the percentage of molecules that satisfy all of the following criteria: Vina < -8.18, QED > 0.25, and SA > 0.59, following [23]. In addition, we introduce molecular reasonability as an extra constraint for defining success. We also evaluate the proportion of molecules that pass all QikProp filters.

Baseline Models. We compare CIDD against a diverse set of 3D-SBDD baselines spanning multiple generative paradigms: the VAE-based **LiGAN** [27]; autoregressive models **AR** [24] and **Pocket2Mol** [25]; and diffusion-based approaches including **TargetDiff** [12], **IPDiff** [15], **DecompDiff** [13], and **TAGMol** [7]. **IPDiff** uses interaction-guided sampling, while **DecompDiff** leverages interaction-aware priors; **TAGMol** adds gradient-based optimization for drug-likeness. We also evaluate **DrugGPS** [37], a fragment-based method, and **MolCRAFT** [26], a Bayesian flow network shown to be state-of-the-art in recent benchmarks [19, 10].

CIDD Settings. We use MolCRAFT in the SBIG step. All modules in the LEDD step are powered by GPT-4o. The Design Module generates 5 candidates per round, and the Selection Module selects the final molecule. For each protein pocket, we generate 10 molecules. All SBIG models are trained on CrossDocked2020 with their released weights.

4.2 General Results

As shown in Table 1, CIDD demonstrates strong overall performance across key drug-likeness metrics—including QED, MRR, SA, and QikProp pass ratio—as well as favorable binding affinity. In comparison, IPDiff, which leverages a trained binding affinity predictor to guide both training and sampling, achieves some improvement in docking scores over TargetDiff. However, it performs worse in terms of MRR, highlighting the potential limitations of focusing solely on binding affinity. Similarly, the gradient-guided method TAGMol aims to enhance multiple properties through predictor guidance during sampling. While TAGMol shows notable improvements in QED, it brings minimal gains and still performs badly in metrics such as MRR and SA, performing comparably to the unguided diffusion model TargetDiff. This suggests that optimization-driven approaches like TAGMol may overfit individual scoring functions rather than learning to generate molecules with generally improved drug-like profiles. In contrast, CIDD delivers **consistent improvements across all major drug-likeness dimensions**, indicating a more robust and comprehensive molecular design capability. These results stem from CIDD's ability to integrate the complementary strengths of distinct modeling paradigms—combining the strong binding affinity modeling capability of 3D generative models with the drug-likeness reasoning and instruction-following power of large language models. Guided by expert-designed prompts and leveraging the LLM's embedded chemical knowledge, CIDD refines molecular structures toward realistic and pharmacologically meaningful candidates. As a result, it achieves a significantly higher success ratio of **34.59%**, compared to **15.72%** for the best

Table 1: **Test Results on CrossDocked2020.** We benchmark several evaluation metrics, including Vina docking score, QED, SA, MRR, success ratio, and QikProp pass ratio. We also report the average molecular weight. Performance ranking per column is color-coded as follows: **best** , second-best

Category	Method	Vina ↓	QED ↑	SA ↑	MRR ↑	Success ↑	QikProp ↑	MW
VAE-based	LiGAN	-6.640	0.394	0.601	59.08%	2.79%	17.37%	286.44
AR-based	AR	-6.737	0.507	0.635	56.67%	3.28%	18.66%	247.50
AR-based	Pocket2Mol	-7.246	0.573	**0.758**	67.88%	14.60%	29.58%	234.30
Diffusion-based	TargetDiff	-7.452	0.474	0.579	37.81%	3.04%	27.63%	346.24
Diff + Inter-Guide	IPDiff	-7.745	0.511	0.627	29.83%	5.31%	25.11%	328.34
Diff + Inter-Prior	DecompDiff	-8.260	0.444	0.609	62.60%	15.72%	29.04%	424.09
Diff + Multi-Guide	TAGMol	-7.563	0.563	0.583	37.31%	3.23%	32.31%	325.50
Fragment-based	DrugGPS	-7.396	0.463	0.622	54.80%	7.17%	25.60%	329.88
BFN-based	MolCRAFT	-7.783	0.503	0.685	58.47%	13.72%	22.37%	325.63
3DSBDD + LLM	CIDD	**-8.496**	**0.576**	0.735	**81.74%**	**34.59%**	**35.22%**	336.70

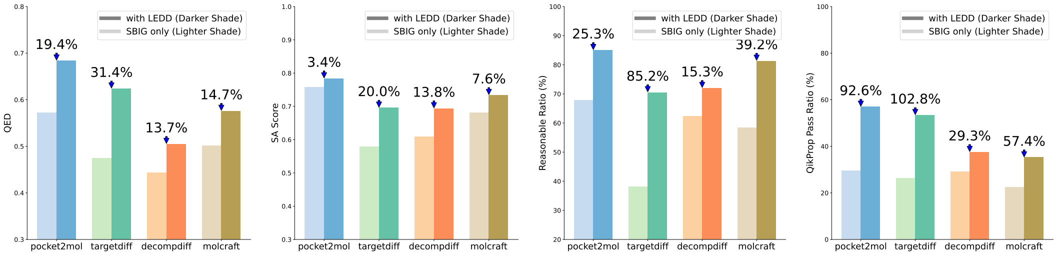

(a) QED (b) SA Score (c) Reasonable Ratio (d) QikProp Pass Ratio

Figure 3: Performance comparison across different metrics indicative of drug potential between models using only SBIG outputs and those incorporating LEDD outputs, evaluated across various 3D-SBDD models as the SBIG module.

baseline—demonstrating its unique capacity to generate molecules that are not only strong binders, but also truly drug-like and synthetically feasible. Interestingly, CIDD achieves comparable QED and SA scores, while significantly outperforming Pocket2Mol in MRR, despite generating molecules that are approximately **50% larger** on average in terms of molecular weight (336.70 vs. 234.30). Moreover, it achieves a substantially better docking score. This result provides strong evidence that CIDD is capable of generating **larger molecules that are still drug-like**, suggesting that its strong performance on drug-likeness metrics is not simply a result of hacking these metrics by producing smaller, simpler molecules.

4.3 Improvements with Different Models on Multiple Metrics

CIDD is a flexible framework designed to interface smoothly with a broad spectrum of 3D SBDD models, significantly enhancing the quality of generated molecules. As illustrated in Figure 3, CIDD brings substantial and consistent improvements across key drug-likeness metrics—including QED, SA Score, Reasonable Ratio, and QikProp Pass Ratio—achieving gains of 31.4%, 20.0%, 85.2%, and 102.8%, respectively. These improvements are observed across different base models, demonstrating CIDD's strong generalization ability and its capacity to enhance diverse, diverse aspects of drug-likeness simultaneously. In contrast to optimization-based methods that often overfit individual metrics, CIDD drives broad and meaningful improvements that reflect a true advancement in the quality of generated drug candidates.

4.4 Ablation and Analysis

Table 2: Ablation studies on LLM variants and pure LLM-based SBDD.

(a) Different LLM Backends in CIDD

LLM	Vina↓	MRR↑	Similarity↑
-	-7.78	58.47%	-
GPT-4o-mini	-8.29	80.02%	0.220
GPT-4o	-8.50	81.37%	0.296
DeepSeek-v3	-8.49	76.00%	0.379
DeepSeek-r1	-8.57	79.17%	0.182

(b) LLM-Only vs. CIDD Comparison

	Vina↓	MRR↑	Success Ratio↑
LLM-SBDD	-6.244	97.45%	5.95%
CIDD-LLM	-7.230	90.97%	17.59%
CIDD	-8.496	81.74%	35.22%

4.4.1 Impact of Different LLMs

We evaluate GPT-4o, GPT-4o-mini, DeepSeek-v3 [5], and DeepSeek-r1 [14] using MolCRAFT as the SBIG module (Table 2a). All models improve drug-likeness metrics (MRR, QikProp) and docking scores. DeepSeek-v3 achieves property gains with minimal edits, while GPT-4o-mini struggles with similarity, and DeepSeek-r1 makes broader, less controllable changes. GPT-4o and DeepSeek-v3 best support CIDD's goal of generating similar yet improved molecules. Smaller models like LLAMA-7B fail to follow design instructions. CIDD remains plug-and-play, benefiting from future LLM advances.

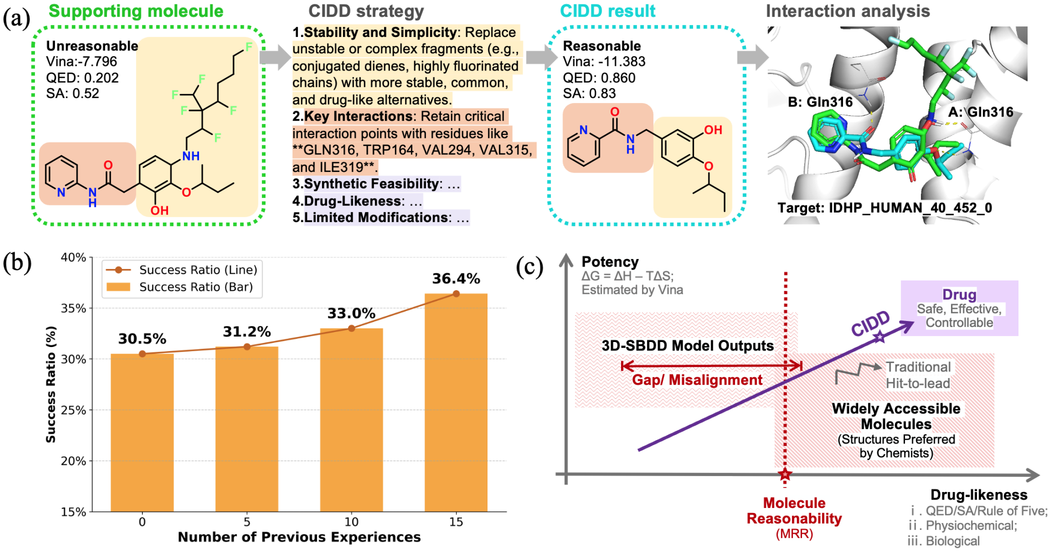

1.**Stability and Simplicity**: Replace unstable or complex fragments (e.g., conjugated dienes, highly fluorinated chains) with more stable, common, and drug-like alternatives.
2.**Key Interactions**: Retain critical interaction points with residues like **GLN316, TRP164, VAL294, VAL315, and ILE319**.
3.**Synthetic Feasibility**: …
4.**Drug-Likeness**: …
5.**Limited Modifications**: …

Figure 4: (a) A generation case and corresponding interpretable design strategy produced by CIDD, resulting in a structurally similar yet better compound. (b) CIDD demonstrates the ability to evolve by leveraging previous design experiences as context, improving generation success rates. (c) CIDD integrates the strengths of 3D-SBDD models and LLMs to enable practical drug design with both high potency and drug-likeness.

4.4.2 Using Pure LLM for SBDD

LLMs alone struggle with 3D protein pocket interpretation in structure-based drug design (SBDD). To test this, we prompted an LLM with PDB-format pocket data and also evaluated CIDD-LLM, which uses LLM-SBDD within the CIDD framework. As shown in Table 2b, LLM-SBDD generates chemically reasonable molecules but performs poorly on binding affinty, leading to a lower success rate than standard CIDD. This highlights the need for combining 3D models' interaction modeling with LLMs' reasoning.

4.5 Advantages and Impact of the CIDD Framework

Interpretable Molecule Design. Figure 4a illustrates the CIDD generation process. The LLM-powered modules analyze and refine the raw supporting molecule (green), producing a high-quality final structure (blue). Problematic fragments—such as an unreasonable diene or an uncommon fluorinated chain—are automatically identified and replaced (e.g., with a benzene ring), while side chains are adjusted to preserve key hydrogen bonds with Gln316 on both Chain A and B. These edits improve docking scores and enhance drug-relevant properties. CIDD performs this refinement through localized fragment substitutions, maintaining the core structure while improving overall drug potential. Notably, the process is inherently **interpretable**: each design step is traceable, with explicit rationales highlighting structural strengths and weaknesses. This transforms conventional opaque SBDD into a transparent, expert-assisting workflow. CIDD also enables the **automated creation of molecule pairs** that differ in drug-likeness with minimal structural edits. These pairs effectively capture how small chemical changes influence pharmaceutical viability, offering high-quality, distributionally aligned data for fine-tuning. Compared to random sampling, they provide more meaningful supervision and help mitigate data scarcity in 3D-SBDD (see Appendix H).

Evolvement Ability. One key advantage of LLMs is their ability to leverage prior experience, provided as context, to generate insightful outputs. To illustrate this, we conducted a proof-of-concept experiment using a relatively lightweight LLM: GPT-4o-mini. The model was given varying numbers of previous design reports and results (0, 5, 10, and 15) as contextual input and tasked with generating insights to support the design module of CIDD. As shown in Figure 4b, the success rate improved as more prior reports were included. These results demonstrate CIDD's capacity for continual evolution by incorporating accumulated experience—without requiring model retraining. This mirrors the way human experts enhance their performance through repeated exposure and practice.

Generating Small Molecules with Both High Potency and Drug-Likeness. Drug potential hinges on two key factors: potency and drug-likeness. While most 3D-SBDD models emphasize target fit, they often produce chemically unreasonable structures. As shown in Figure 4c, our **CIDD** framework bridges this gap by combining geometric modeling with LLM-driven reasoning. The LLM not only corrects unfavorable fragments but also plans coherent molecular edits that balance multiple objectives. By coordinating spatial and chemical constraints within a unified generation process, CIDD effectively overcomes the traditional trade-off between interaction strength and drug-likeness.

5 Conclusion

We presented **CIDD**, a collaborative framework that unifies 3D interaction modeling and LLM-driven reasoning for structure-based drug design. CIDD addresses a key limitation of current generative models: the tendency to generate interaction-compatible but chemically unreasonable molecules. Through a modular, interpretable generation process, CIDD achieves state-of-the-art results on the CrossDocked2020 benchmark—substantially improving drug-likeness metrics (QED, SA, MRR, QikProp) while maintaining high binding affinity. By bridging 3D geometric modeling with language-guided design, our approach sets a foundation for future directions in rational, interpretable, and generalizable drug generation. We envision such a collaborative paradigm enabling broader tasks such as target discovery and hit-to-lead optimization in early-stage drug discovery.

Acknowledgements

This work is supported by Beijing Academy of Artificial Intelligence and Beijing Frontier Research Center for Biological Structure Fundings.

References

[1] Asad Aali, Adney Cardoza, and Melissa Capo. Splitwiser: Efficient lm inference with constrained resources. *arXiv preprint arXiv:2505.03763*, 2025.

[2] Josh Achiam, Steven Adler, Sandhini Agarwal, Lama Ahmad, Ilge Akkaya, Florencia Leoni Aleman, Diogo Almeida, Janko Altenschmidt, Sam Altman, Shyamal Anadkat, et al. Gpt-4 technical report. *arXiv preprint arXiv:2303.08774*, 2023.

[3] G Richard Bickerton, Gaia V Paolini, Jérémy Besnard, Sorel Muresan, and Andrew L Hopkins. Quantifying the chemical beauty of drugs. *Nature chemistry*, 4(2):90–98, 2012.

[4] Chiranjib Chakraborty, Manojit Bhattacharya, and Sang-Soo Lee. Artificial intelligence enabled chatgpt and large language models in drug target discovery, drug discovery, and development. *Molecular Therapy-Nucleic Acids*, 33:866–868, 2023.

[5] DeepSeek-AI, Aixin Liu, Bei Feng, Bing Xue, Bingxuan Wang, Bochao Wu, Chengda Lu, Chenggang Zhao, Chengqi Deng, Chenyu Zhang, Chong Ruan, Damai Dai, Daya Guo, Dejian Yang, Deli Chen, Dongjie Ji, Erhang Li, Fangyun Lin, Fucong Dai, Fuli Luo, Guangbo Hao, Guanting Chen, Guowei Li, H. Zhang, Han Bao, Hanwei Xu, Haocheng Wang, Haowei Zhang, Honghui Ding, Huajian Xin, Huazuo Gao, Hui Li, Hui Qu, J. L. Cai, Jian Liang, Jianzhong Guo, Jiaqi Ni, Jiashi Li, Jiawei Wang, Jin Chen, Jingchang Chen, Jingyang Yuan, Junjie Qiu, Junlong Li, Junxiao Song, Kai Dong, Kai Hu, Kaige Gao, Kang Guan, Kexin Huang, Kuai Yu, Lean Wang, Lecong Zhang, Lei Xu, Leyi Xia, Liang Zhao, Litong Wang, Liyue Zhang, Meng Li, Miaojun Wang, Mingchuan Zhang, Minghua Zhang, Minghui Tang, Mingming Li, Ning Tian, Panpan Huang, Peiyi Wang, Peng Zhang, Qiancheng Wang, Qihao Zhu, Qinyu Chen, Qiushi Du, R. J. Chen, R. L. Jin, Ruiqi Ge, Ruisong Zhang, Ruizhe Pan, Runji Wang, Runxin Xu, Ruoyu Zhang, Ruyi Chen, S. S. Li, Shanghao Lu, Shangyan Zhou, Shanhuang Chen, Shaoqing Wu, Shengfeng Ye, Shengfeng Ye, Shirong Ma, Shiyu Wang, Shuang Zhou, Shuiping Yu, Shunfeng Zhou, Shuting Pan, T. Wang, Tao Yun, Tian Pei, Tianyu Sun, W. L. Xiao, Wangding Zeng, Wanjia Zhao, Wei An, Wen Liu, Wenfeng Liang, Wenjun Gao, Wenqin Yu, Wentao Zhang, X. Q. Li, Xiangyue Jin, Xianzu Wang, Xiao Bi, Xiaodong Liu, Xiaohan Wang, Xiaojin Shen, Xiaokang Chen, Xiaokang Zhang, Xiaosha Chen, Xiaotao Nie, Xiaowen Sun, Xiaoxiang Wang, Xin Cheng, Xin Liu, Xin Xie, Xingchao Liu, Xingkai Yu, Xinnan Song, Xinxia Shan, Xinyi

Zhou, Xinyu Yang, Xinyuan Li, Xuecheng Su, Xuheng Lin, Y. K. Li, Y. Q. Wang, Y. X. Wei, Y. X. Zhu, Yang Zhang, Yanhong Xu, Yanhong Xu, Yanping Huang, Yao Li, Yao Zhao, Yaofeng Sun, Yaohui Li, Yaohui Wang, Yi Yu, Yi Zheng, Yichao Zhang, Yifan Shi, Yiliang Xiong, Ying He, Ying Tang, Yishi Piao, Yisong Wang, Yixuan Tan, Yiyang Ma, Yiyuan Liu, Yongqiang Guo, Yu Wu, Yuan Ou, Yuchen Zhu, Yuduan Wang, Yue Gong, Yuheng Zou, Yujia He, Yukun Zha, Yunfan Xiong, Yunxian Ma, Yuting Yan, Yuxiang Luo, Yuxiang You, Yuxuan Liu, Yuyang Zhou, Z. F. Wu, Z. Z. Ren, Zehui Ren, Zhangli Sha, Zhe Fu, Zhean Xu, Zhen Huang, Zhen Zhang, Zhenda Xie, Zhengyan Zhang, Zhewen Hao, Zhibin Gou, Zhicheng Ma, Zhigang Yan, Zhihong Shao, Zhipeng Xu, Zhiyu Wu, Zhongyu Zhang, Zhuoshu Li, Zihui Gu, Zijia Zhu, Zijun Liu, Zilin Li, Ziwei Xie, Ziyang Song, Ziyi Gao, and Zizheng Pan. Deepseek-v3 technical report, 2024.

[6] Jorg Degen, Christof Wegscheid-Gerlach, Andrea Zaliani, and Matthias Rarey. On the art of compiling and using'drug-like'chemical fragment spaces. *ChemMedChem*, 3(10):1503, 2008.

[7] Vineeth Dorna, D Subhalingam, Keshav Kolluru, Shreshth Tuli, Mrityunjay Singh, Saurabh Singal, NM Krishnan, and Sayan Ranu. Tagmol: Target-aware gradient-guided molecule generation. *arXiv preprint arXiv:2406.01650*, 2024.

[8] Peter Ertl and Ansgar Schuffenhauer. Estimation of synthetic accessibility score of drug-like molecules based on molecular complexity and fragment contributions. *Journal of cheminformatics*, 1:1–11, 2009.

[9] Paul G Francoeur, Tomohide Masuda, Jocelyn Sunseri, Andrew Jia, Richard B Iovanisci, Ian Snyder, and David R Koes. Three-dimensional convolutional neural networks and a cross-docked data set for structure-based drug design. *Journal of chemical information and modeling*, 60(9):4200–4215, 2020.

[10] Bowen Gao, Haichuan Tan, Yanwen Huang, Minsi Ren, Xiao Huang, Wei-Ying Ma, Ya-Qin Zhang, and Yanyan Lan. Reframing structure-based drug design model evaluation via metrics correlated to practical needs. In *The Thirteenth International Conference on Learning Representations*.

[11] Team GLM, Aohan Zeng, Bin Xu, Bowen Wang, Chenhui Zhang, Da Yin, Dan Zhang, Diego Rojas, Guanyu Feng, Hanlin Zhao, et al. Chatglm: A family of large language models from glm-130b to glm-4 all tools. *arXiv preprint arXiv:2406.12793*, 2024.

[12] Jiaqi Guan, Wesley Wei Qian, Xingang Peng, Yufeng Su, Jian Peng, and Jianzhu Ma. 3d equivariant diffusion for target-aware molecule generation and affinity prediction. *arXiv preprint arXiv:2303.03543*, 2023.

[13] Jiaqi Guan, Xiangxin Zhou, Yuwei Yang, Yu Bao, Jian Peng, Jianzhu Ma, Qiang Liu, Liang Wang, and Quanquan Gu. Decompdiff: diffusion models with decomposed priors for structure-based drug design. *arXiv preprint arXiv:2403.07902*, 2024.

[14] Daya Guo, Dejian Yang, Haowei Zhang, Junxiao Song, Ruoyu Zhang, Runxin Xu, Qihao Zhu, Shirong Ma, Peiyi Wang, Xiao Bi, et al. Deepseek-r1: Incentivizing reasoning capability in llms via reinforcement learning. *arXiv preprint arXiv:2501.12948*, 2025.

[15] Zhilin Huang, Ling Yang, Xiangxin Zhou, Zhilong Zhang, Wentao Zhang, Xiawu Zheng, Jie Chen, Yu Wang, Bin Cui, and Wenming Yang. Protein-ligand interaction prior for binding-aware 3d molecule diffusion models. In *The Twelfth International Conference on Learning Representations*, 2024.

[16] Leukothea Ioakimidis, Loizos Thoukydidis, Amin Mirza, Saira Naeem, and Johannes Reynisson. Benchmarking the reliability of qikprop. correlation between experimental and predicted values. *QSAR & Combinatorial Science*, 27(4):445–456, 2008.

[17] Craig Knox, Mike Wilson, Christen M Klinger, Mark Franklin, Eponine Oler, Alex Wilson, Allison Pon, Jordan Cox, Na Eun Chin, Seth A Strawbridge, et al. Drugbank 6.0: the drugbank knowledgebase for 2024. *Nucleic acids research*, 52(D1):D1265–D1275, 2024.

[18] Woosuk Kwon, Zhuohan Li, Siyuan Zhuang, Ying Sheng, Lianmin Zheng, Cody Hao Yu, Joseph Gonzalez, Hao Zhang, and Ion Stoica. Efficient memory management for large language model serving with pagedattention. In *Proceedings of the 29th symposium on operating systems principles*, pages 611–626, 2023.

[19] Haitao Lin, Guojiang Zhao, Odin Zhang, Yufei Huang, Lirong Wu, Zicheng Liu, Siyuan Li, Cheng Tan, Zhifeng Gao, and Stan Z Li. Cbgbench: fill in the blank of protein-molecule complex binding graph. *arXiv preprint arXiv:2406.10840*, 2024.

[20] Christopher A Lipinski, Franco Lombardo, Beryl W Dominy, and Paul J Feeney. Experimental and computational approaches to estimate solubility and permeability in drug discovery and development settings. *Advanced drug delivery reviews*, 64:4–17, 2012.

[21] Aixin Liu, Bei Feng, Bin Wang, Bingxuan Wang, Bo Liu, Chenggang Zhao, Chengqi Dengr, Chong Ruan, Damai Dai, Daya Guo, et al. Deepseek-v2: A strong, economical, and efficient mixture-of-experts language model. *arXiv preprint arXiv:2405.04434*, 2024.

[22] Shengchao Liu, Jiongxiao Wang, Yijin Yang, Chengpeng Wang, Ling Liu, Hongyu Guo, and Chaowei Xiao. Conversational drug editing using retrieval and domain feedback. In *The twelfth international conference on learning representations*, 2024.

[23] Siyu Long, Yi Zhou, Xinyu Dai, and Hao Zhou. Zero-shot 3d drug design by sketching and generating. *Advances in Neural Information Processing Systems*, 35:23894–23907, 2022.

[24] Shitong Luo, Jiaqi Guan, Jianzhu Ma, and Jian Peng. A 3d generative model for structure-based drug design. *Advances in Neural Information Processing Systems*, 34:6229–6239, 2021.

[25] Xingang Peng, Shitong Luo, Jiaqi Guan, Qi Xie, Jian Peng, and Jianzhu Ma. Pocket2mol: Efficient molecular sampling based on 3d protein pockets. In *International Conference on Machine Learning*, pages 17644–17655. PMLR, 2022.

[26] Yanru Qu, Keyue Qiu, Yuxuan Song, Jingjing Gong, Jiawei Han, Mingyue Zheng, Hao Zhou, and Wei-Ying Ma. Molcraft: Structure-based drug design in continuous parameter space. *arXiv preprint arXiv:2404.12141*, 2024.

[27] Matthew Ragoza, Tomohide Masuda, and David Ryan Koes. Generating 3d molecules conditional on receptor binding sites with deep generative models. *Chemical science*, 13(9):2701–2713, 2022.

[28] Raimond BG Ravelli, Benoît Gigant, Patrick A Curmi, Isabelle Jourdain, Sylvie Lachkar, André Sobel, and Marcel Knossow. Insight into tubulin regulation from a complex with colchicine and a stathmin-like domain. *Nature*, 428(6979):198–202, 2004.

[29] David Rogers and Mathew Hahn. Extended-connectivity fingerprints. *Journal of chemical information and modeling*, 50(5):742–754, 2010.

[30] Schrödinger, LLC. *QikProp*. Schrödinger, LLC, New York, NY, 2025. Schrödinger Release 2021-2.

[31] Yuxuan Song, Zheng Zhang, Cheng Luo, Pengyang Gao, Fan Xia, Hao Luo, Zheng Li, Yuehang Yang, Hongli Yu, Xingwei Qu, et al. Seed diffusion: A large-scale diffusion language model with high-speed inference. *arXiv preprint arXiv:2508.02193*, 2025.

[32] Bart L Staker, Michael D Feese, Mark Cushman, Yves Pommier, David Zembower, Lance Stewart, and Alex B Burgin. Structures of three classes of anticancer agents bound to the human topoisomerase i- dna covalent complex. *Journal of medicinal chemistry*, 48(7):2336–2345, 2005.

[33] Hugo Touvron, Thibaut Lavril, Gautier Izacard, Xavier Martinet, Marie-Anne Lachaux, Timothée Lacroix, Baptiste Rozière, Naman Goyal, Eric Hambro, Faisal Azhar, et al. Llama: Open and efficient foundation language models. *arXiv preprint arXiv:2302.13971*, 2023.

[34] Oleg Trott and Arthur J Olson. Autodock vina: improving the speed and accuracy of docking with a new scoring function, efficient optimization, and multithreading. *Journal of computational chemistry*, 31(2):455–461, 2010.

[35] Xiaolun Wang, Shelley Allen, James F Blake, Vickie Bowcut, David M Briere, Andrew Calinisan, Joshua R Dahlke, Jay B Fell, John P Fischer, Robin J Gunn, et al. Identification of mrtx1133, a noncovalent, potent, and selective krasg12d inhibitor. *Journal of medicinal chemistry*, 65(4):3123–3133, 2021.

[36] Jiale Xu, Rui Zhang, Cong Guo, Weiming Hu, Zihan Liu, Feiyang Wu, Yu Feng, Shixuan Sun, Changxu Shao, Yuhong Guo, et al. vtensor: Flexible virtual tensor management for efficient llm serving. *arXiv preprint arXiv:2407.15309*, 2024.

[37] Zaixi Zhang and Qi Liu. Learning subpocket prototypes for generalizable structure-based drug design. In *International Conference on Machine Learning*, pages 41382–41398. PMLR, 2023.

A Discussion on the Pharmaceutical Terminology

In this work, we employ a comprehensive set of evaluation metrics—**Vina**, **QED**, **SA**, our proposed **MRR**, the **Success Ratio**, and **QikProp**—to analyze different facets of molecular generation performance. Following established practices, we use Vina scores to assess the 3D complementarity between generated molecules and their target binding sites. Meanwhile, we evaluate broader molecular properties using standard metrics (QED and SA), the domain-informed MRR, and physicochemical and pharmacokinetic descriptors from QikProp, which are widely used in computer-aided drug design (CADD).

To clarify the key concepts underpinning our evaluation framework, we distinguish among **drug potential**, **drug-likeness**, **molecular reasonability**, and **chemical validity**.

Previous studies have often focused too narrowly on geometric complementarity, overlooking other essential requirements a drug-like molecule must fulfill. We introduce the term *drug potential* to describe the overall suitability of a molecule as a drug candidate, encompassing not only binding affinity but also synthetic accessibility, chemical stability, pharmacokinetics (absorption, distribution, metabolism, and excretion), and safety. These properties are intrinsically determined by molecular structure and collectively influence whether a molecule can reach its intended biological target and survive the drug development process.

The term *drug-likeness* is widely used in medicinal chemistry to reflect the multidimensional suitability of a molecule as a drug candidate. Drug discovery and development (DDD), however, are deeply influenced by human expertise—including implicit preferences for molecular scaffolds and nuanced, often tacit, domain knowledge that is difficult to formalize or quantify. As a result, even experienced medicinal chemists struggle to define or approximate the true probability function $p(\text{drug})$, which represents the likelihood that a molecule will become a viable therapeutic candidate. However, the machine learning community often oversimplifies *drug-likeness* to metrics such as QED or Lipinski's Rule of Five, which capture only a narrow range of basic physicochemical properties. This simplification overlooks critical factors such as oral bioavailability, metabolic stability, and toxicity risks (e.g., hERG liability).

At a more fundamental level, a molecule must be *chemically valid*, meaning it adheres to basic chemical rules such as proper valence and atom types. However, we observe that many model-generated molecules—while technically valid—contain rare or unstable structural substructures that would be flagged by human medicinal chemists. These structures are neither common nor practically accessible and thus fall outside the bounds of what is typically accepted in pharmaceutical research. Despite the central importance of this distinction, prior work has not proposed an effective metric to differentiate between chemically plausible structures and those that are formally valid but unrealistic. To fill this gap, we propose MRR, a rule-based metric that reflects medicinal chemistry heuristics. It identifies implausible features such as unstable ring systems and uncommon conjugation patterns, offering an interpretable and practical means of identifying unrealistic model outputs.

By explicitly defining these concepts and introducing MRR, we aim to guide molecular generation efforts toward pharmaceutically meaningful directions, bridging the gap between computational outputs and real-world drug development feasibility.

B Limitations

One limitation of CIDD is its dependence on pretrained LLMs, which may occasionally introduce hallucinations in underexplored chemical regions.

C Detailed Prompts and Responses for LEDD

In this section, we present the detailed workflow of the CIDD framework, including the prompts and example responses for each module.

Figure 5 illustrates the complete drug design pipeline. The Interaction Module first identifies key fragments within the supporting molecule that interact with the protein pocket. This information is then utilized by the Design Module, which devises strategies to replace uncommon or unfavorable fragments while preserving crucial interactions. Once a new molecule is designed, the Evaluation

Phase within the Design Module assesses its viability. Finally, the Reflection Module analyzes the design process and outcomes, highlighting both strengths and areas for improvement.

Figure 6 presents the prompt and example response for the Interaction Analysis Module.

Figures 7 and 8 display the prompt and example response for the Design Module.

Figures 9, 10, and 11 illustrate the prompt and example responses for the Reflection Module.

Figures 12 and 13 show the prompt and example response for the Selection Module.

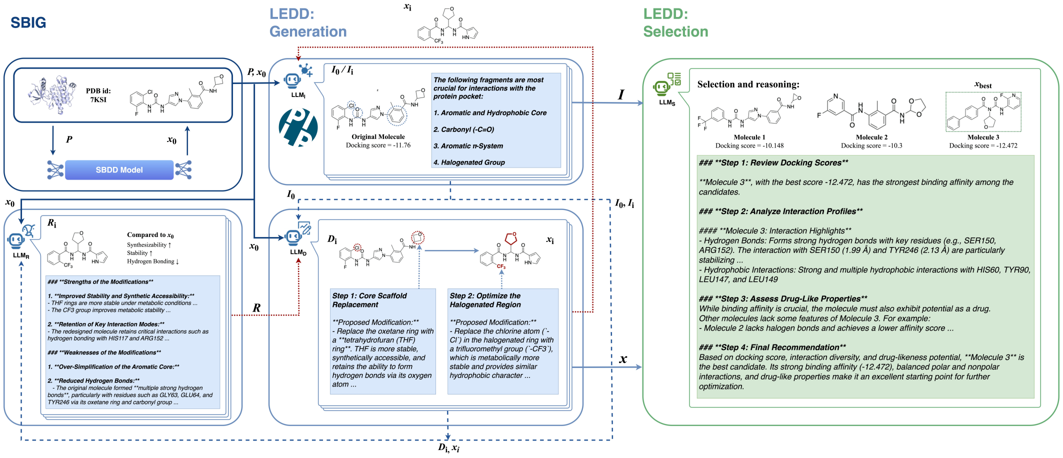

```
The following fragments are most
crucial for interactions with the
protein pocket:

1. Aromatic and Hydrophobic Core

2. Carbonyl (-C=O)

3. Aromatic π-System

4. Halogenated Group
```

```
### **Strengths of the Modifications**

1. **Improved Stability and Synthetic Accessibility:**
- THF rings are more stable under metabolic conditions ...
- The CF3 group improves metabolic stability ...

2. **Retention of Key Interaction Modes:**
- The redesigned molecule retains critical interactions such as
hydrogen bonding with HIS117 and ARG152 ...

### **Weaknesses of the Modifications**

1. **Over-Simplification of the Aromatic Core:**

2. **Reduced Hydrogen Bonds:**
  - The original molecule formed **multiple strong hydrogen
bonds**, particularly with residues such as GLY63, GLU64, and
TYR246 via its oxetane ring and carbonyl group ...
```

```
Step 1: Core Scaffold
Replacement

**Proposed Modification:**
- Replace the oxetane ring with
a **tetrahydrofuran (THF)
ring**. THF is more stable,
synthetically accessible, and
retains the ability to form
hydrogen bonds via its oxygen
atom ...
```

```
Step 2: Optimize the
Halogenated Region

**Proposed Modification:**
- Replace the chlorine atom (`-
Cl`) in the halogenated ring with
a trifluoromethyl group (`-CF3`),
which is metabolically more
stable and provides similar
hydrophobic character ...
```

```
### **Step 1: Review Docking Scores**

**Molecule 3**, with the best score -12.472, has the strongest binding affinity among the
candidates.

### **Step 2: Analyze Interaction Profiles**

#### **Molecule 3: Interaction Highlights**
- Hydrogen Bonds: Forms strong hydrogen bonds with key residues (e.g., SER150,
ARG152). The interaction with SER150 (1.99 Å) and TYR246 (2.13 Å) are particularly
stabilizing ...
- Hydrophobic Interactions: Strong and multiple hydrophobic interactions with HIS60, TYR90,
LEU147, and LEU149

### **Step 3: Assess Drug-Like Properties**
While binding affinity is crucial, the molecule must also exhibit potential as a drug.
Other molecules lack some features of Molecule 3. For example:
- Molecule 2 lacks halogen bonds and achieves a lower affinity score ...

### **Step 4: Final Recommendation**
Based on docking score, interaction diversity, and drug-likeness potential, **Molecule 3** is
the best candidate. Its strong binding affinity (-12.472), balanced polar and nonpolar
interactions, and drug-like properties make it an excellent starting point for further
optimization.
```

Figure 5: Workflow of CIDD framework

Interaction analysis

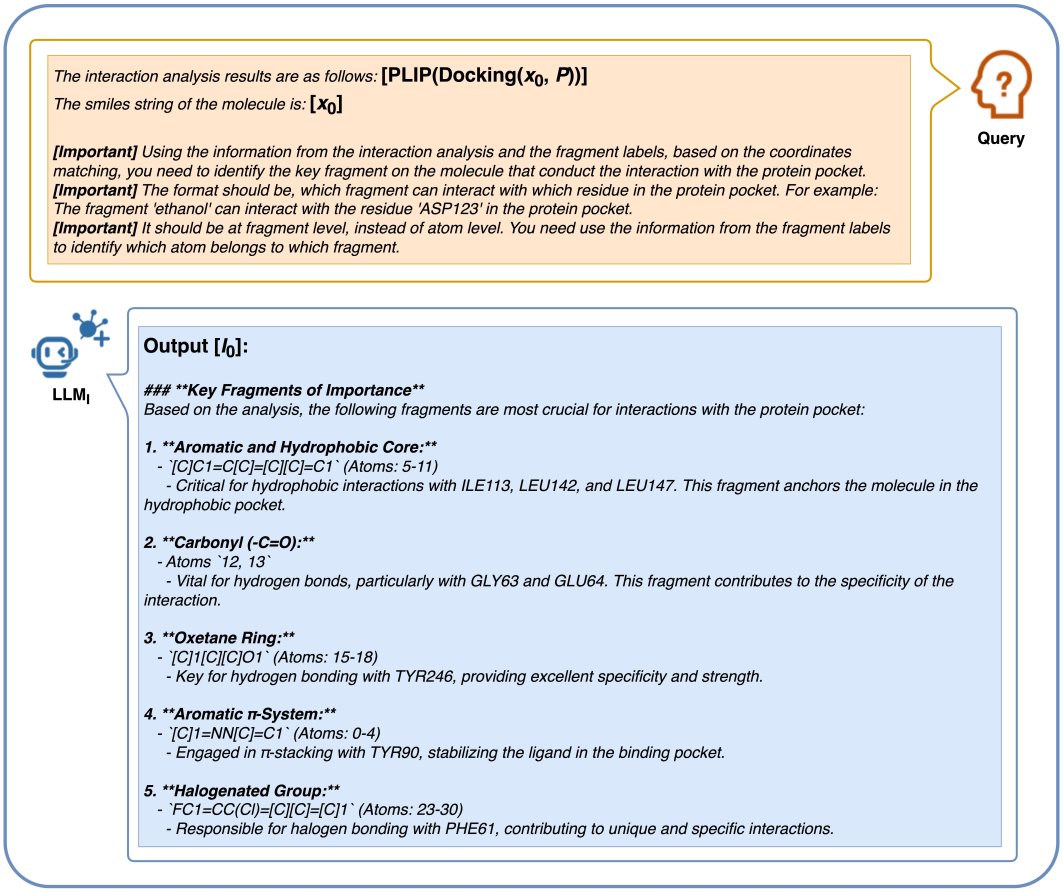
Query
LLM_I

The interaction analysis results are as follows: **[PLIP(Docking(x_0, P))]**
The smiles string of the molecule is: **[x_0]**

[Important] *Using the information from the interaction analysis and the fragment labels, based on the coordinates matching, you need to identify the key fragment on the molecule that conduct the interaction with the protein pocket.*
[Important] *The format should be, which fragment can interact with which residue in the protein pocket. For example: The fragment 'ethanol' can interact with the residue 'ASP123' in the protein pocket.*
[Important] *It should be at fragment level, instead of atom level. You need use the information from the fragment labels to identify which atom belongs to which fragment.*

Output [l_0]:

*### **Key Fragments of Importance***
Based on the analysis, the following fragments are most crucial for interactions with the protein pocket:

*1. **Aromatic and Hydrophobic Core:***
- `[C]C1=C[C]=[C][C]=C1` (Atoms: 5-11)
- Critical for hydrophobic interactions with ILE113, LEU142, and LEU147. This fragment anchors the molecule in the hydrophobic pocket.

*2. **Carbonyl (-C=O):***
- Atoms `12, 13`
- Vital for hydrogen bonds, particularly with GLY63 and GLU64. This fragment contributes to the specificity of the interaction.

*3. **Oxetane Ring:***
- `[C]1[C][C]O1` (Atoms: 15-18)
- Key for hydrogen bonding with TYR246, providing excellent specificity and strength.

*4. **Aromatic π-System:***
- `[C]1=NN[C]=C1` (Atoms: 0-4)
- Engaged in π-stacking with TYR90, stabilizing the ligand in the binding pocket.

*5. **Halogenated Group:***
- `FC1=CC(Cl)=[C][C]=[C]1` (Atoms: 23-30)
- Responsible for halogen bonding with PHE61, contributing to unique and specific interactions.

Figure 6: Interaction analysis module

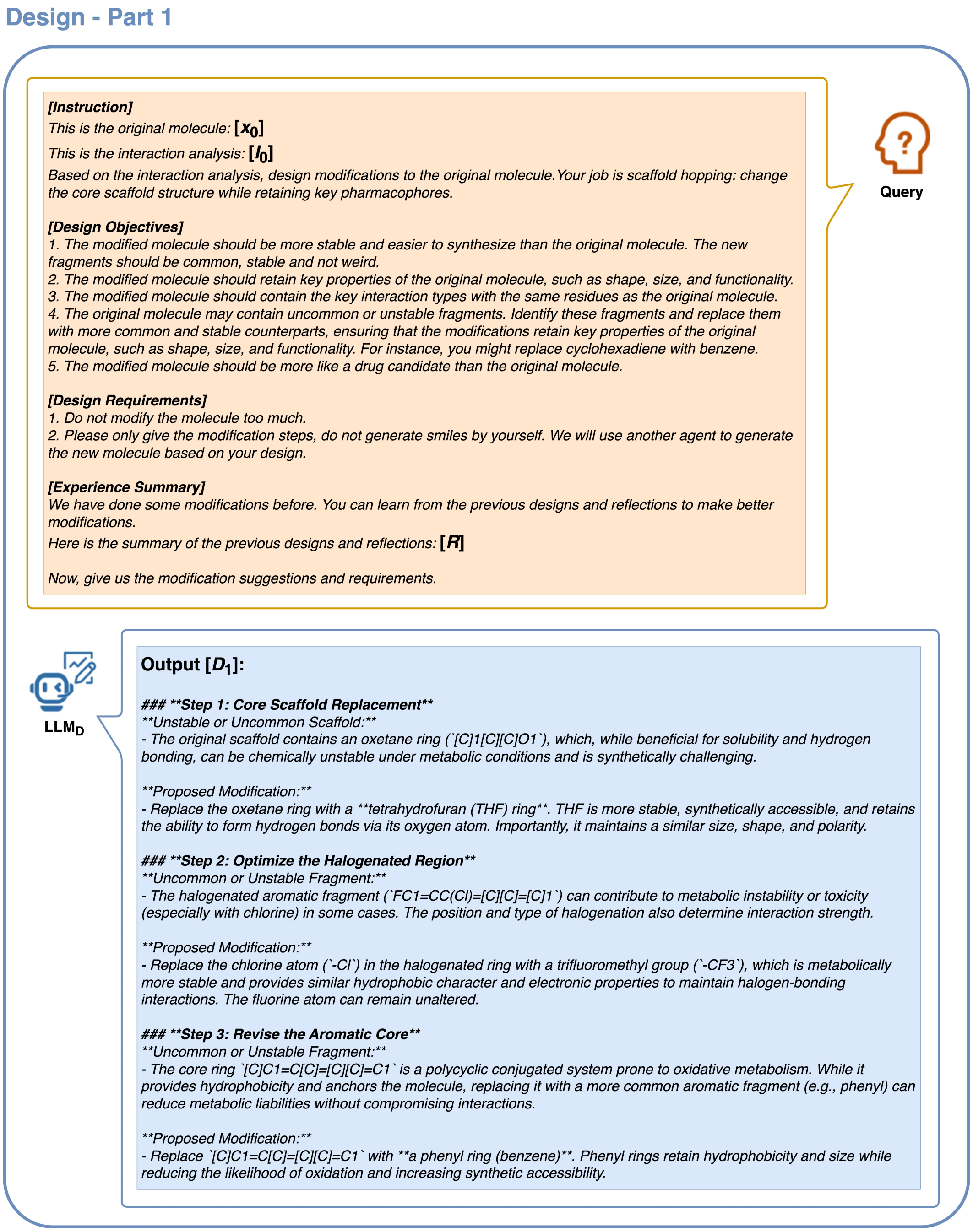

Design - Part 1

[Instruction]

This is the original molecule: **[x_0]**

This is the interaction analysis: **[I_0]**

Based on the interaction analysis, design modifications to the original molecule.Your job is scaffold hopping: change the core scaffold structure while retaining key pharmacophores.

[Design Objectives]

1. The modified molecule should be more stable and easier to synthesize than the original molecule. The new fragments should be common, stable and not weird.
2. The modified molecule should retain key properties of the original molecule, such as shape, size, and functionality.
3. The modified molecule should contain the key interaction types with the same residues as the original molecule.
4. The original molecule may contain uncommon or unstable fragments. Identify these fragments and replace them with more common and stable counterparts, ensuring that the modifications retain key properties of the original molecule, such as shape, size, and functionality. For instance, you might replace cyclohexadiene with benzene.
5. The modified molecule should be more like a drug candidate than the original molecule.

[Design Requirements]

1. Do not modify the molecule too much.
2. Please only give the modification steps, do not generate smiles by yourself. We will use another agent to generate the new molecule based on your design.

[Experience Summary]

We have done some modifications before. You can learn from the previous designs and reflections to make better modifications.

Here is the summary of the previous designs and reflections: **[R]**

Now, give us the modification suggestions and requirements.

Output [D_1]:

*### **Step 1: Core Scaffold Replacement***
Unstable or Uncommon Scaffold:
- The original scaffold contains an oxetane ring (`[C]1[C][C]O1`), which, while beneficial for solubility and hydrogen bonding, can be chemically unstable under metabolic conditions and is synthetically challenging.

Proposed Modification:
*- Replace the oxetane ring with a **tetrahydrofuran (THF) ring**. THF is more stable, synthetically accessible, and retains the ability to form hydrogen bonds via its oxygen atom. Importantly, it maintains a similar size, shape, and polarity.*

*### **Step 2: Optimize the Halogenated Region***
Uncommon or Unstable Fragment:
- The halogenated aromatic fragment (`FC1=CC(Cl)=[C][C]=[C]1`) can contribute to metabolic instability or toxicity (especially with chlorine) in some cases. The position and type of halogenation also determine interaction strength.

Proposed Modification:
- Replace the chlorine atom (`-Cl`) in the halogenated ring with a trifluoromethyl group (`-CF3`), which is metabolically more stable and provides similar hydrophobic character and electronic properties to maintain halogen-bonding interactions. The fluorine atom can remain unaltered.

*### **Step 3: Revise the Aromatic Core***
Uncommon or Unstable Fragment:
- The core ring `[C]C1=C[C]=[C][C]=C1` is a polycyclic conjugated system prone to oxidative metabolism. While it provides hydrophobicity and anchors the molecule, replacing it with a more common aromatic fragment (e.g., phenyl) can reduce metabolic liabilities without compromising interactions.

Proposed Modification:
*- Replace `[C]C1=C[C]=[C][C]=C1` with **a phenyl ring (benzene)**. Phenyl rings retain hydrophobicity and size while reducing the likelihood of oxidation and increasing synthetic accessibility.*

Figure 7: Design Module

Design - Part 2

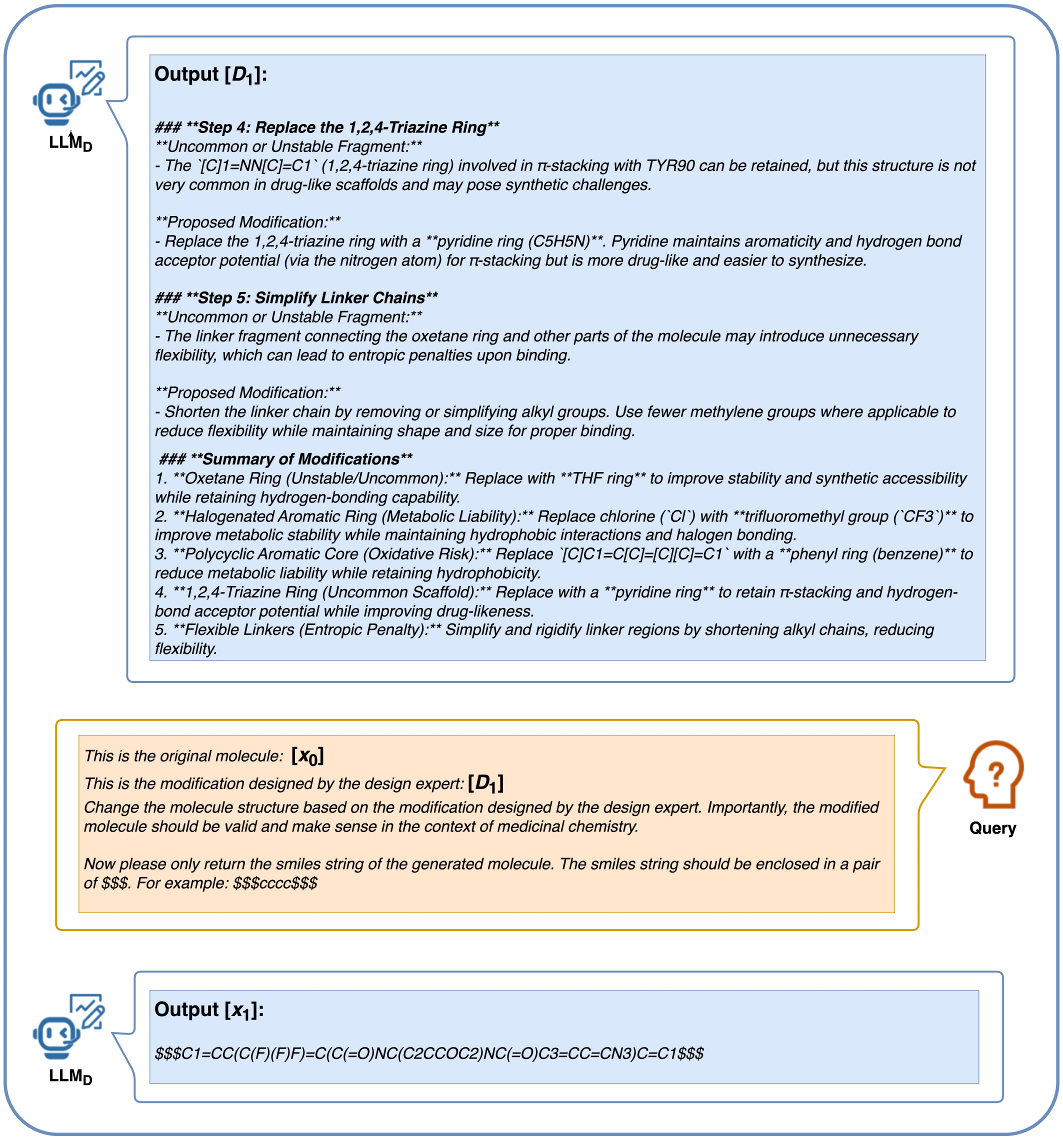

Output [D_1]:

*### **Step 4: Replace the 1,2,4-Triazine Ring***
Uncommon or Unstable Fragment:
- The `[C]1=NN[C]=C1` (1,2,4-triazine ring) involved in π-stacking with TYR90 can be retained, but this structure is not very common in drug-like scaffolds and may pose synthetic challenges.

Proposed Modification:
*- Replace the 1,2,4-triazine ring with a **pyridine ring (C5H5N)**. Pyridine maintains aromaticity and hydrogen bond acceptor potential (via the nitrogen atom) for π-stacking but is more drug-like and easier to synthesize.*

*### **Step 5: Simplify Linker Chains***
Uncommon or Unstable Fragment:
- The linker fragment connecting the oxetane ring and other parts of the molecule may introduce unnecessary flexibility, which can lead to entropic penalties upon binding.

Proposed Modification:
- Shorten the linker chain by removing or simplifying alkyl groups. Use fewer methylene groups where applicable to reduce flexibility while maintaining shape and size for proper binding.

*### **Summary of Modifications***
*1. **Oxetane Ring (Unstable/Uncommon):** Replace with **THF ring** to improve stability and synthetic accessibility while retaining hydrogen-bonding capability.*
*2. **Halogenated Aromatic Ring (Metabolic Liability):** Replace chlorine (`Cl`) with **trifluoromethyl group (`CF3`)** to improve metabolic stability while maintaining hydrophobic interactions and halogen bonding.*
*3. **Polycyclic Aromatic Core (Oxidative Risk):** Replace `[C]C1=C[C]=[C][C]=C1` with a **phenyl ring (benzene)** to reduce metabolic liability while retaining hydrophobicity.*
*4. **1,2,4-Triazine Ring (Uncommon Scaffold):** Replace with a **pyridine ring** to retain π-stacking and hydrogen-bond acceptor potential while improving drug-likeness.*
*5. **Flexible Linkers (Entropic Penalty):** Simplify and rigidify linker regions by shortening alkyl chains, reducing flexibility.*

This is the original molecule: **[x_0]**
This is the modification designed by the design expert: **[D_1]**
Change the molecule structure based on the modification designed by the design expert. Importantly, the modified molecule should be valid and make sense in the context of medicinal chemistry.

Now please only return the smiles string of the generated molecule. The smiles string should be enclosed in a pair of $$$. For example: $$$cccc$$$

Output [x_1]:

$$$C1=CC(C(F)(F)F)=C(C(=O)NC(C2CCOC2)NC(=O)C3=CC=CN3)C=C1$$$

Figure 8: Design Module

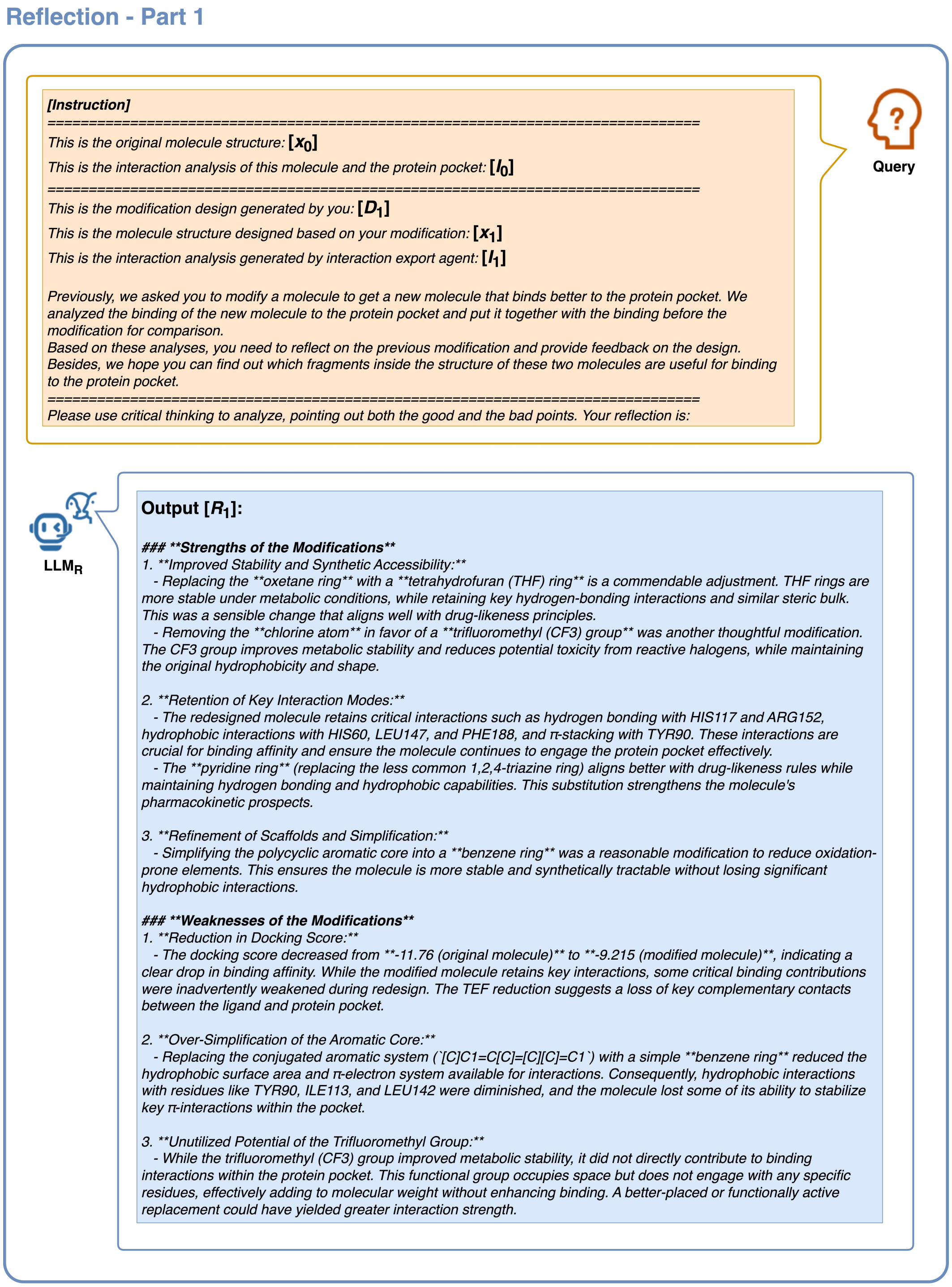

[Instruction]

==

This is the original molecule structure: **[x_0]**

This is the interaction analysis of this molecule and the protein pocket: **[I_0]**

==

This is the modification design generated by you: **[D_1]**

This is the molecule structure designed based on your modification: **[x_1]**

This is the interaction analysis generated by interaction export agent: **[I_1]**

Previously, we asked you to modify a molecule to get a new molecule that binds better to the protein pocket. We analyzed the binding of the new molecule to the protein pocket and put it together with the binding before the modification for comparison.
Based on these analyses, you need to reflect on the previous modification and provide feedback on the design.
Besides, we hope you can find out which fragments inside the structure of these two molecules are useful for binding to the protein pocket.

==

Please use critical thinking to analyze, pointing out both the good and the bad points. Your reflection is:

Output [R_1]:

### **Strengths of the Modifications**
*1. **Improved Stability and Synthetic Accessibility:***
*- Replacing the **oxetane ring** with a **tetrahydrofuran (THF) ring** is a commendable adjustment. THF rings are more stable under metabolic conditions, while retaining key hydrogen-bonding interactions and similar steric bulk. This was a sensible change that aligns well with drug-likeness principles.*
*- Removing the **chlorine atom** in favor of a **trifluoromethyl (CF3) group** was another thoughtful modification. The CF3 group improves metabolic stability and reduces potential toxicity from reactive halogens, while maintaining the original hydrophobicity and shape.*

*2. **Retention of Key Interaction Modes:***
- The redesigned molecule retains critical interactions such as hydrogen bonding with HIS117 and ARG152, hydrophobic interactions with HIS60, LEU147, and PHE188, and π-stacking with TYR90. These interactions are crucial for binding affinity and ensure the molecule continues to engage the protein pocket effectively.
*- The **pyridine ring** (replacing the less common 1,2,4-triazine ring) aligns better with drug-likeness rules while maintaining hydrogen bonding and hydrophobic capabilities. This substitution strengthens the molecule's pharmacokinetic prospects.*

*3. **Refinement of Scaffolds and Simplification:***
*- Simplifying the polycyclic aromatic core into a **benzene ring** was a reasonable modification to reduce oxidation-prone elements. This ensures the molecule is more stable and synthetically tractable without losing significant hydrophobic interactions.*

### **Weaknesses of the Modifications**
*1. **Reduction in Docking Score:***
*- The docking score decreased from **-11.76 (original molecule)** to **-9.215 (modified molecule)**, indicating a clear drop in binding affinity. While the modified molecule retains key interactions, some critical binding contributions were inadvertently weakened during redesign. The TEF reduction suggests a loss of key complementary contacts between the ligand and protein pocket.*

*2. **Over-Simplification of the Aromatic Core:***
*- Replacing the conjugated aromatic system (\`[C]C1=C[C]=[C][C]=C1\`) with a simple **benzene ring** reduced the hydrophobic surface area and π-electron system available for interactions. Consequently, hydrophobic interactions with residues like TYR90, ILE113, and LEU142 were diminished, and the molecule lost some of its ability to stabilize key π-interactions within the pocket.*

*3. **Unutilized Potential of the Trifluoromethyl Group:***
- While the trifluoromethyl (CF3) group improved metabolic stability, it did not directly contribute to binding interactions within the protein pocket. This functional group occupies space but does not engage with any specific residues, effectively adding to molecular weight without enhancing binding. A better-placed or functionally active replacement could have yielded greater interaction strength.

Figure 9: Reflection Module

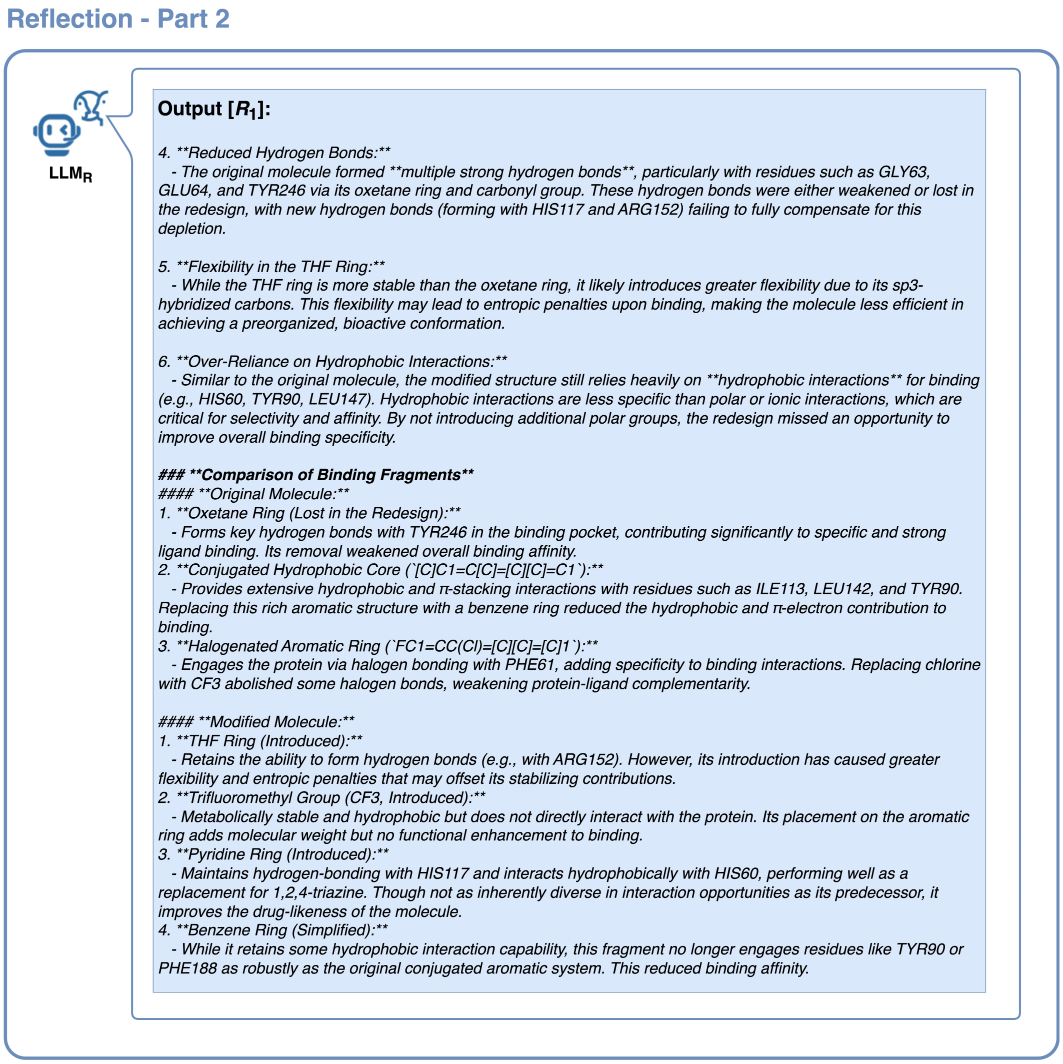

Reflection - Part 2

Output [R_1]:

4. **Reduced Hydrogen Bonds:**
   - The original molecule formed **multiple strong hydrogen bonds**, particularly with residues such as GLY63, GLU64, and TYR246 via its oxetane ring and carbonyl group. These hydrogen bonds were either weakened or lost in the redesign, with new hydrogen bonds (forming with HIS117 and ARG152) failing to fully compensate for this depletion.

5. **Flexibility in the THF Ring:**
   - While the THF ring is more stable than the oxetane ring, it likely introduces greater flexibility due to its sp3-hybridized carbons. This flexibility may lead to entropic penalties upon binding, making the molecule less efficient in achieving a preorganized, bioactive conformation.

6. **Over-Reliance on Hydrophobic Interactions:**
   - Similar to the original molecule, the modified structure still relies heavily on **hydrophobic interactions** for binding (e.g., HIS60, TYR90, LEU147). Hydrophobic interactions are less specific than polar or ionic interactions, which are critical for selectivity and affinity. By not introducing additional polar groups, the redesign missed an opportunity to improve overall binding specificity.

Comparison of Binding Fragments
Original Molecule:
1. **Oxetane Ring (Lost in the Redesign):**
   - Forms key hydrogen bonds with TYR246 in the binding pocket, contributing significantly to specific and strong ligand binding. Its removal weakened overall binding affinity.
2. **Conjugated Hydrophobic Core (`[C]C1=C[C]=[C][C]=C1`):**
   - Provides extensive hydrophobic and π-stacking interactions with residues such as ILE113, LEU142, and TYR90. Replacing this rich aromatic structure with a benzene ring reduced the hydrophobic and π-electron contribution to binding.
3. **Halogenated Aromatic Ring (`FC1=CC(Cl)=[C][C]=[C]1`):**
   - Engages the protein via halogen bonding with PHE61, adding specificity to binding interactions. Replacing chlorine with CF3 abolished some halogen bonds, weakening protein-ligand complementarity.

Modified Molecule:
1. **THF Ring (Introduced):**
   - Retains the ability to form hydrogen bonds (e.g., with ARG152). However, its introduction has caused greater flexibility and entropic penalties that may offset its stabilizing contributions.
2. **Trifluoromethyl Group (CF3, Introduced):**
   - Metabolically stable and hydrophobic but does not directly interact with the protein. Its placement on the aromatic ring adds molecular weight but no functional enhancement to binding.
3. **Pyridine Ring (Introduced):**
   - Maintains hydrogen-bonding with HIS117 and interacts hydrophobically with HIS60, performing well as a replacement for 1,2,4-triazine. Though not as inherently diverse in interaction opportunities as its predecessor, it improves the drug-likeness of the molecule.
4. **Benzene Ring (Simplified):**
   - While it retains some hydrophobic interaction capability, this fragment no longer engages residues like TYR90 or PHE188 as robustly as the original conjugated aromatic system. This reduced binding affinity.

Figure 10: Reflection Module

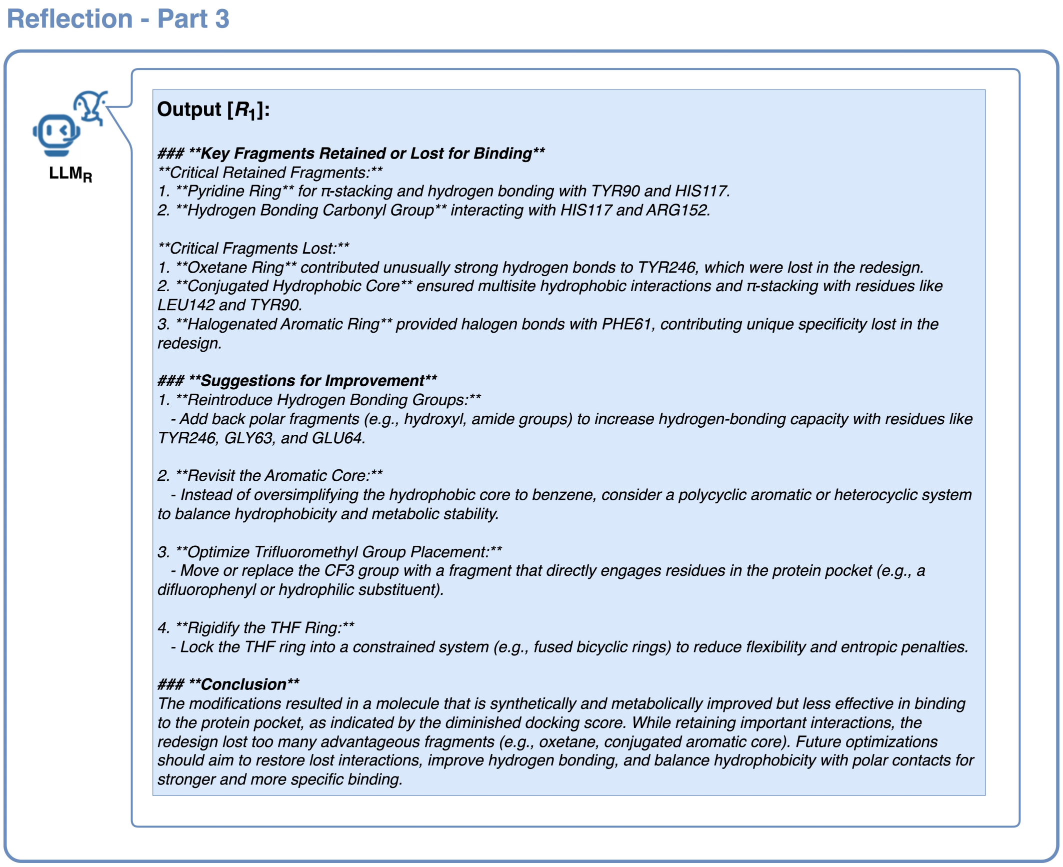

Reflection - Part 3

LLM_R

Output [R_1]:

```
### **Key Fragments Retained or Lost for Binding**
**Critical Retained Fragments:**
1. **Pyridine Ring** for π-stacking and hydrogen bonding with TYR90 and HIS117.
2. **Hydrogen Bonding Carbonyl Group** interacting with HIS117 and ARG152.

**Critical Fragments Lost:**
1. **Oxetane Ring** contributed unusually strong hydrogen bonds to TYR246, which were lost in the redesign.
2. **Conjugated Hydrophobic Core** ensured multisite hydrophobic interactions and π-stacking with residues like LEU142 and TYR90.
3. **Halogenated Aromatic Ring** provided halogen bonds with PHE61, contributing unique specificity lost in the redesign.

### **Suggestions for Improvement**
1. **Reintroduce Hydrogen Bonding Groups:**
   - Add back polar fragments (e.g., hydroxyl, amide groups) to increase hydrogen-bonding capacity with residues like TYR246, GLY63, and GLU64.

2. **Revisit the Aromatic Core:**
   - Instead of oversimplifying the hydrophobic core to benzene, consider a polycyclic aromatic or heterocyclic system to balance hydrophobicity and metabolic stability.

3. **Optimize Trifluoromethyl Group Placement:**
   - Move or replace the CF3 group with a fragment that directly engages residues in the protein pocket (e.g., a difluorophenyl or hydrophilic substituent).

4. **Rigidify the THF Ring:**
   - Lock the THF ring into a constrained system (e.g., fused bicyclic rings) to reduce flexibility and entropic penalties.

### **Conclusion**
The modifications resulted in a molecule that is synthetically and metabolically improved but less effective in binding to the protein pocket, as indicated by the diminished docking score. While retaining important interactions, the redesign lost too many advantageous fragments (e.g., oxetane, conjugated aromatic core). Future optimizations should aim to restore lost interactions, improve hydrogen bonding, and balance hydrophobicity with polar contacts for stronger and more specific binding.
```

Figure 11: Reflection Module

Selection - Part 1

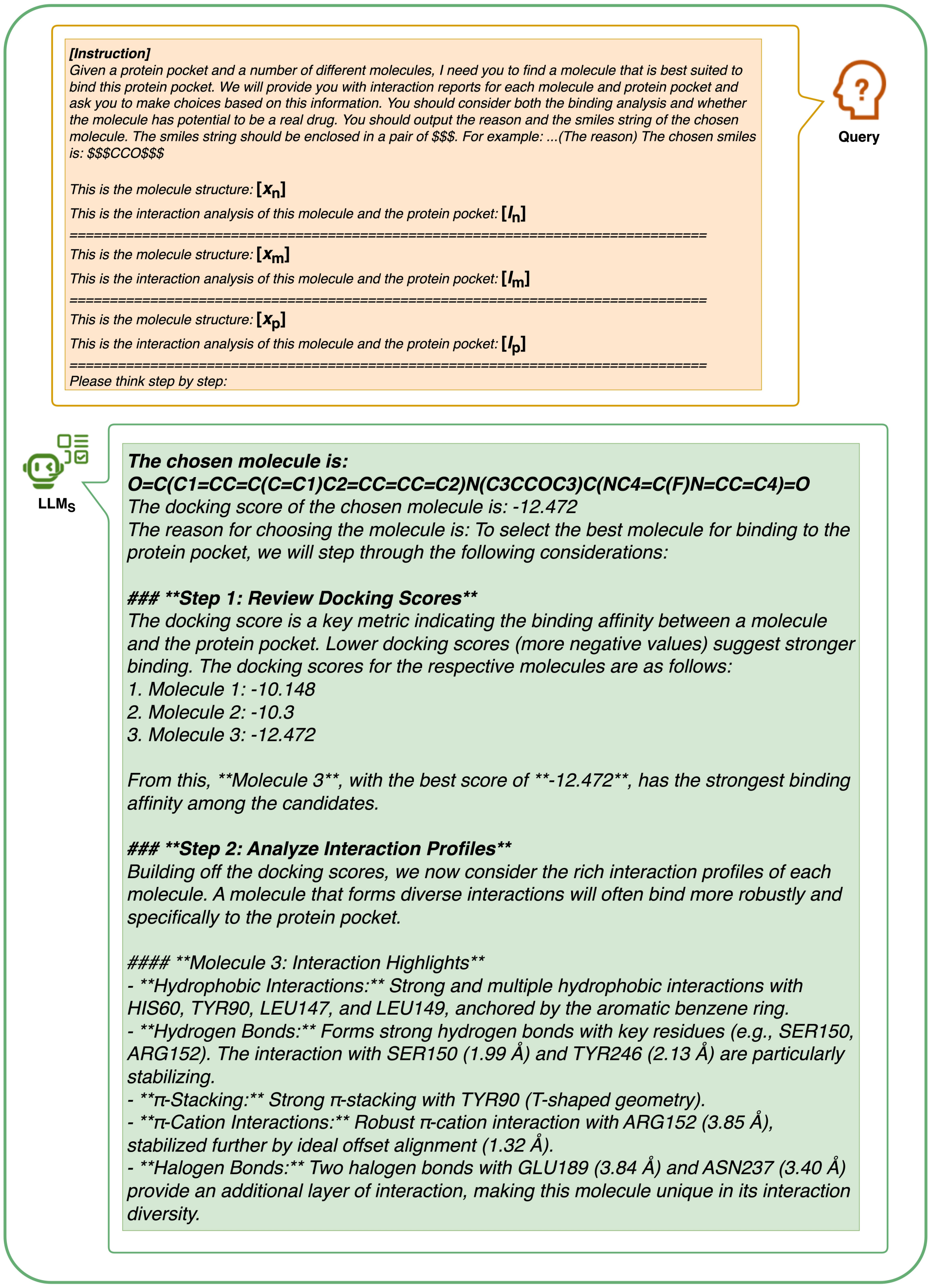

[Instruction]

Given a protein pocket and a number of different molecules, I need you to find a molecule that is best suited to bind this protein pocket. We will provide you with interaction reports for each molecule and protein pocket and ask you to make choices based on this information. You should consider both the binding analysis and whether the molecule has potential to be a real drug. You should output the reason and the smiles string of the chosen molecule. The smiles string should be enclosed in a pair of $$$. For example: ...(The reason) The chosen smiles is: $$$CCO$$$

This is the molecule structure: $[x_n]$

This is the interaction analysis of this molecule and the protein pocket: $[I_n]$

==

This is the molecule structure: $[x_m]$

This is the interaction analysis of this molecule and the protein pocket: $[I_m]$

==

This is the molecule structure: $[x_p]$

This is the interaction analysis of this molecule and the protein pocket: $[I_p]$

==

Please think step by step:

The chosen molecule is:
O=C(C1=CC=C(C=C1)C2=CC=CC=C2)N(C3CCOC3)C(NC4=C(F)N=CC=C4)=O
The docking score of the chosen molecule is: -12.472
The reason for choosing the molecule is: To select the best molecule for binding to the protein pocket, we will step through the following considerations:

### **Step 1: Review Docking Scores**
The docking score is a key metric indicating the binding affinity between a molecule and the protein pocket. Lower docking scores (more negative values) suggest stronger binding. The docking scores for the respective molecules are as follows:
1. Molecule 1: -10.148
2. Molecule 2: -10.3
3. Molecule 3: -12.472

*From this, **Molecule 3**, with the best score of **-12.472**, has the strongest binding affinity among the candidates.*

### **Step 2: Analyze Interaction Profiles**
Building off the docking scores, we now consider the rich interaction profiles of each molecule. A molecule that forms diverse interactions will often bind more robustly and specifically to the protein pocket.

*#### **Molecule 3: Interaction Highlights***
*- **Hydrophobic Interactions:** Strong and multiple hydrophobic interactions with HIS60, TYR90, LEU147, and LEU149, anchored by the aromatic benzene ring.*
*- **Hydrogen Bonds:** Forms strong hydrogen bonds with key residues (e.g., SER150, ARG152). The interaction with SER150 (1.99 Å) and TYR246 (2.13 Å) are particularly stabilizing.*
*- **π-Stacking:** Strong π-stacking with TYR90 (T-shaped geometry).*
*- **π-Cation Interactions:** Robust π-cation interaction with ARG152 (3.85 Å), stabilized further by ideal offset alignment (1.32 Å).*
*- **Halogen Bonds:** Two halogen bonds with GLU189 (3.84 Å) and ASN237 (3.40 Å) provide an additional layer of interaction, making this molecule unique in its interaction diversity.*

Figure 12: Selection Module

Selection - Part 2

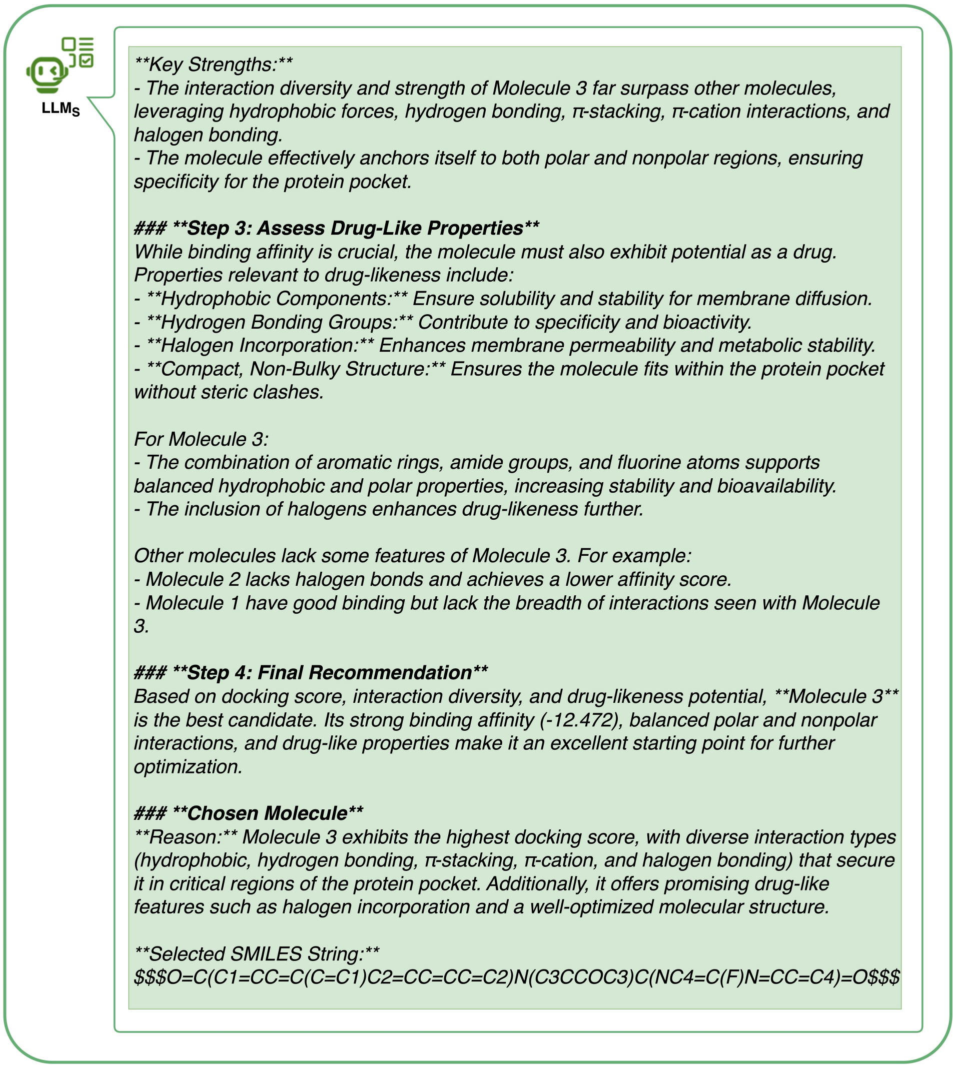

Key Strengths:
- The interaction diversity and strength of Molecule 3 far surpass other molecules, leveraging hydrophobic forces, hydrogen bonding, π-stacking, π-cation interactions, and halogen bonding.
- The molecule effectively anchors itself to both polar and nonpolar regions, ensuring specificity for the protein pocket.

Step 3: Assess Drug-Like Properties
While binding affinity is crucial, the molecule must also exhibit potential as a drug. Properties relevant to drug-likeness include:
- **Hydrophobic Components:** Ensure solubility and stability for membrane diffusion.
- **Hydrogen Bonding Groups:** Contribute to specificity and bioactivity.
- **Halogen Incorporation:** Enhances membrane permeability and metabolic stability.
- **Compact, Non-Bulky Structure:** Ensures the molecule fits within the protein pocket without steric clashes.

For Molecule 3:
- The combination of aromatic rings, amide groups, and fluorine atoms supports balanced hydrophobic and polar properties, increasing stability and bioavailability.
- The inclusion of halogens enhances drug-likeness further.

Other molecules lack some features of Molecule 3. For example:
- Molecule 2 lacks halogen bonds and achieves a lower affinity score.
- Molecule 1 have good binding but lack the breadth of interactions seen with Molecule 3.

Step 4: Final Recommendation
Based on docking score, interaction diversity, and drug-likeness potential, **Molecule 3** is the best candidate. Its strong binding affinity (-12.472), balanced polar and nonpolar interactions, and drug-like properties make it an excellent starting point for further optimization.

Chosen Molecule
Reason: Molecule 3 exhibits the highest docking score, with diverse interaction types (hydrophobic, hydrogen bonding, π-stacking, π-cation, and halogen bonding) that secure it in critical regions of the protein pocket. Additionally, it offers promising drug-like features such as halogen incorporation and a well-optimized molecular structure.

Selected SMILES String:
$$$O=C(C1=CC=C(C=C1)C2=CC=CC=C2)N(C3CCOC3)C(NC4=C(F)N=CC=C4)=O$$$

Figure 13: Selection Module

D Algorithm for MRR and AUR

The complete calculation process for assessing the reasonability of a molecule is outlined in Algorithm 1.

Algorithm 1: Evaluation of Molecular Reasonability

```
Input: Molecule object (mol)
Output: Molecular Reasonability (MRR) and Atom Unreasonable Ratio (AUR)
Step 1: Detect Carbonyl and Imine Group Carbons
Initialize an empty list for carbonyl/imine carbons.
foreach bond in mol do
    if bond is double and one atom is carbon, the other is oxygen or nitrogen then
        Record the carbon atom in carbonyl/imine groups.
Step 2: Identification of Ring Systems
Identify all ring structures and their corresponding atom indices within mol.
Calculate the number of atoms in each ring.
foreach ring in the molecule do
    if the ring shares one or more atoms with another ring then
        Group the connected rings into a single ring system.
Step 3: Evaluation of Molecular Reasonability
Exclude any atoms previously identified as part of carbonyl or imine groups.
Classify the remaining carbon atoms in each ring system as follows:
        • $sp^2$ hybridized: Aromatic or unsaturated carbons.
        • Non-$sp^2$ hybridized: Saturated carbons.
foreach ring system in the ring systems do
    if the ring system contains multiple rings and all carbon atoms are non-$sp^2$ then
        Mark the molecule as unreasonable.
        Add the atoms to the unreasonable atom list.
foreach ring system in the remaining ring systems do
    foreach ring in the ring system do
        if all carbon atoms within the ring are consistent in hybridization (either all $sp^2$ or all
        non-$sp^2$) then
            Mark the ring as reasonable.
        else
            Add the ring to the remaining ring list.
while the remaining ring list is not empty do
    foreach ring in the remaining ring list do
        Exclude atoms that have already been classified as reasonable.
        if all remaining carbon atoms are consistent in hybridization (either all $sp^2$ or all
        non-$sp^2$) then
            Mark the ring as reasonable.
    if no new reasonable rings are identified then
        Mark the molecule as unreasonable.
        Add the carbon atoms in the remaining rings to the unreasonable atom list.
        Exit the loop.
Calculate AUR as the ratio of unreasonable atom count to the total ring atom count.
Return MRR and AUR.
```

E QikProp properties

The full set of properties used for the QikProp pass ratio analysis is presented in Table 3.

The QikProp filter applied in the main text incorporates a comprehensive range of criteria provided by QikProp, including "#stars", "#amine", "#amidine", "#acid", "#amide", "#rotor", "#rtvFG", "mol_MW", "dipole", "SASA", "FOSA", "FISA", "PISA", "WPSA", "volume", "donorHB", "acceptHB", "dip$^2/V$", "ACxDN·$5/$SA", "glob", "QPpolrz", "QPlogPC16", "QPlogPoct", "QPlogPw", "QPlogPo/w", "QPlogS", "CIQPlogS", "QPPCaco", "QPlogBB", "QPPMDCK", "QPlogKp", "IP(eV)", "EA(eV)", "#metab", "QPlogKhsa", "PercentHumanOralAbsorption", "SAFluorine", "SAamideO", "PSA", "#NandO", and "RuleOfThree".

Table 3: QikProp Properties and Descriptors

Property or Descriptor	**Description**	**Range or Recommended Values**
Molecule name	The molecule's identifier derived from the title line in the input structure file. If no title is provided, the file name is used.	
#stars	Count of descriptors or properties falling outside the 95% range for known drugs. A higher count indicates reduced drug-likeness.	0 – 5
#amine	Total non-conjugated amine groups present in the molecule.	0 – 1
#amidine	Number of amidine or guanidine functional groups in the structure.	0
#acid	Quantity of carboxylic acid groups in the molecule.	0 – 1
#amide	Count of non-conjugated amide groups.	0 – 1
#rotor	Number of rotatable bonds that are neither trivial nor sterically hindered.	0 – 15
#rtvFG	Total reactive functional groups present in the molecule, potentially affecting stability or toxicity.	0 – 2
mol_MW	Molecular weight of the compound.	130.0 – 725.0
Dipole	Calculated dipole moment of the molecule in Debye units.	1.0 – 12.5
SASA	Solvent-accessible surface area (SASA) in square angstroms, measured with a probe of 1.4 Å radius.	300.0 – 1000.0
FOSA	Hydrophobic part of the SASA, representing saturated carbon and attached hydrogen atoms.	0.0 – 750.0
FISA	Hydrophilic fraction of the SASA, encompassing polar atoms like nitrogen and oxygen.	7.0 – 330.0
PISA	SASA component attributable to π-systems.	0.0 – 450.0
WPSA	Weakly polar component of the SASA, including atoms like halogens, phosphorus, and sulfur.	0.0 – 175.0
Volume	Total solvent-accessible volume in cubic angstroms, determined with a 1.4 Å radius probe.	500.0 – 2000.0
donorHB	Estimated number of hydrogen bonds donated to water in solution.	0.0 – 6.0
accptHB	Estimated number of hydrogen bonds accepted from water.	2.0 – 20.0
Dip^2/V	Dipole moment squared divided by molecular volume, a key factor in solvation energy.	0.0 – 0.13
ACxDN$^{0.5}$/SA	Cohesive interaction index in solids based on molecular properties.	0.0 – 0.05
glob	Descriptor measuring how close the shape of a molecule is to a sphere.	0.75 – 0.95
QPpolrz	Predicted molecular polarizability in cubic angstroms.	13.0 – 70.0
QPlogPC16	Predicted partition coefficient between hexadecane and gas phases.	4.0 – 18.0
QPlogPoct	Predicted partition coefficient between octanol and gas phases.	8.0 – 35.0
QPlogPw	Predicted partition coefficient between water and gas phases.	4.0 – 45.0
QPlogPo/w	Predicted partition coefficient between octanol and water phases.	-2.0 – 6.5
QPlogS	Predicted solubility of the molecule in water (log S, in mol/L).	-6.5 – 0.5
CIQPlogS	Conformation-independent prediction of water solubility (log S).	-6.5 – 0.5
QPPCaco	Predicted permeability through Caco-2 cells, in nm/s.	<25 poor, >500 great
QPlogBB	Predicted partition coefficient for brain/blood.	-3.0 – 1.2
QPPMDCK	Predicted permeability through MDCK cells, in nm/s.	<25 poor, >500 great
QPlogKp	Predicted skin permeability (log Kp).	-8.0 – -1.0
IP(eV)	Ionization potential calculated using PM3.	7.9 – 10.5
EA(eV)	Electron affinity calculated using PM3.	-0.9 – 1.7
#metab	Predicted number of possible metabolic reactions.	1 – 8
QPlogKhsa	Predicted binding affinity to human serum albumin.	-1.5 – 1.5
HumanOralAbsorption	Qualitative assessment of oral absorption: 1 (low), 2 (medium), or 3 (high).	
PercentHumanOralAbsorption	Quantitative prediction of oral absorption percentage.	>80% high, <25% poor
SAFluorine	Solvent-accessible fluorine surface area.	0.0 – 100.0
SAamideO	Solvent-accessible surface area of amide oxygen atoms.	0.0 – 35.0
PSA	Polar surface area, calculated for nitrogen, oxygen, and carbonyl groups.	7.0 – 200.0
#NandO	Total count of nitrogen and oxygen atoms.	2 – 15
RuleOfFive	Number of Lipinski's Rule of Five violations.	Max 4
RuleOfThree	Number of Jorgensen's Rule of Three violations.	Max 3
#ringatoms	Count of atoms within molecular rings.	
#in34	Number of atoms in 3- or 4-membered rings.	
#in56	Number of atoms in 5- or 6-membered rings.	
#noncon	Number of ring atoms unable to form conjugated aromatic systems.	
#nonHatm	Count of heavy (non-hydrogen) atoms in the structure.	
Jm	Predicted maximum transdermal transport rate (μg cm^{-2} hr^{-1}).	

F Computing Resource

In this work, we primarily utilize pretrained 3D generative models and large language model (LLM) APIs to conduct our experiments. The 3D model sampling is performed using a single NVIDIA A100 GPU. For the LLM component, we rely on API-based access provided by the service provider, which requires no local computational resources.

G More Experiment Results

Based on the different criteria presented in Table 3, we provide additional pass ratio results in Table 4.

Filter 1 is identical to the QikProp filter used in the main text.

Filter 2 removes some non-essential properties and focuses on well-defined physicochemical properties, including "#rtvFG", "QPlogS", "QPlogPo/w", "mol_MW", "dipole", "SASA", "FOSA", "FISA", "IP(eV)", "EA(eV)", "#metab", "PercentHumanOralAbsorption", and "PSA".

Filter 3 assesses molecular compliance with the "RuleOfFive" criterion. However, instead of allowing up to four violations as typically recommended, this filter adopts a stricter definition, considering only molecules that fully comply (i.e., setting the maximum allowable violations to zero).

Table 4: QikProp results for different methods with and without CIDD

Method	Filter 1	Filter 2	Filter 3
Pocket2Mol			
Original	29.58%	51.52%	89.58%
CIDD	56.97%	75.64%	92.24%
TargetDiff			
Original	26.32%	48.20%	69.47%
CIDD	53.37%	75.60%	81.85%
DecompDiff			
Original	29.04%	53.96%	55.14%
CIDD	37.54%	68.48%	65.64%
MolCRAFT			
Original	22.37%	43.52%	66.45%
CIDD	35.22%	63.23%	74.09%

H More cases

More generated molecules from CIDD are presented below. For each case, we display the initial supporting molecule derived from 3D-SBDD models alongside the final designed molecules produced by CIDD.

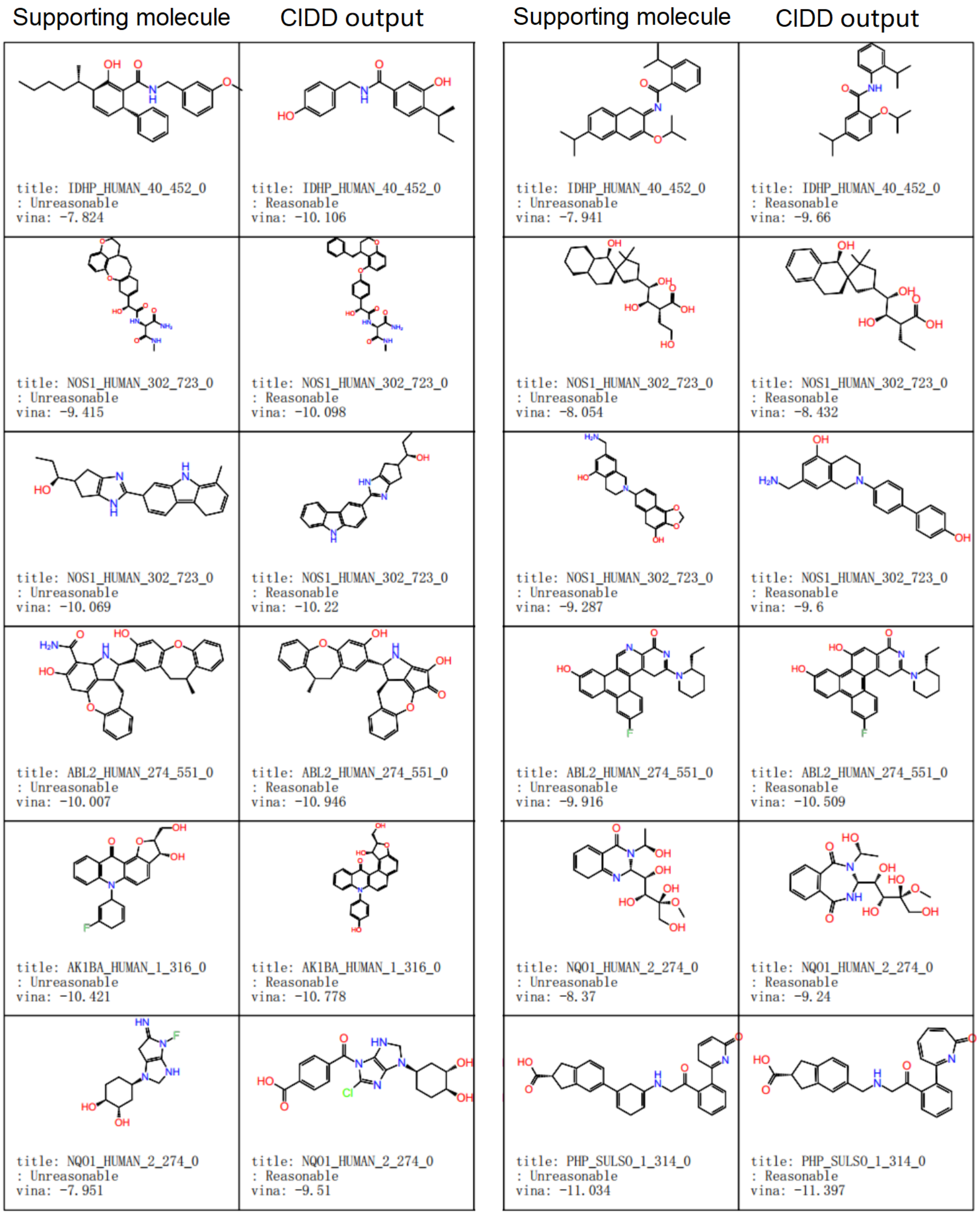
Supporting molecule
CIDD output
Supporting molecule
CIDD output
title: IDHP_HUMAN_40_452_0 : Unreasonable vina: -7.824
title: IDHP_HUMAN_40_452_0 : Reasonable vina: -10.106
title: IDHP_HUMAN_40_452_0 : Unreasonable vina: -7.941
title: IDHP_HUMAN_40_452_0 : Reasonable vina: -9.66
title: NOS1_HUMAN_302_723_0 : Unreasonable vina: -9.415
title: NOS1_HUMAN_302_723_0 : Reasonable vina: -10.098
title: NOS1_HUMAN_302_723_0 : Unreasonable vina: -8.054
title: NOS1_HUMAN_302_723_0 : Reasonable vina: -8.432
title: NOS1_HUMAN_302_723_0 : Unreasonable vina: -10.069
title: NOS1_HUMAN_302_723_0 : Reasonable vina: -10.22
title: NOS1_HUMAN_302_723_0 : Unreasonable vina: -9.287
title: NOS1_HUMAN_302_723_0 : Reasonable vina: -9.6
title: ABL2_HUMAN_274_551_0 : Unreasonable vina: -10.007
title: ABL2_HUMAN_274_551_0 : Reasonable vina: -10.946
title: ABL2_HUMAN_274_551_0 : Unreasonable vina: -9.916
title: ABL2_HUMAN_274_551_0 : Reasonable vina: -10.509
title: AK1BA_HUMAN_1_316_0 : Unreasonable vina: -10.421
title: AK1BA_HUMAN_1_316_0 : Reasonable vina: -10.778
title: NQO1_HUMAN_2_274_0 : Unreasonable vina: -8.37
title: NQO1_HUMAN_2_274_0 : Reasonable vina: -9.24
title: NQO1_HUMAN_2_274_0 : Unreasonable vina: -7.951
title: NQO1_HUMAN_2_274_0 : Reasonable vina: -9.51
title: PHP_SULSO_1_314_0 : Unreasonable vina: -11.034
title: PHP_SULSO_1_314_0 : Reasonable vina: -11.397

Supporting molecule	CIDD output
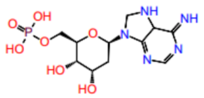 title: PHKG1_RABIT_6_296_ATPsite_0 : Unreasonable vina: -8. 548	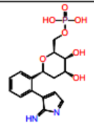 title: PHKG1_RABIT_6_296_ATPsite_0 : Reasonable vina: -8. 727
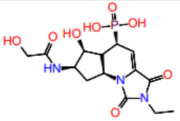 title: CD38_HUMAN_44_300_0 : Unreasonable vina: -7. 443	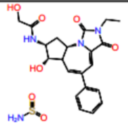 title: CD38_HUMAN_44_300_0 : Reasonable vina: -8. 863
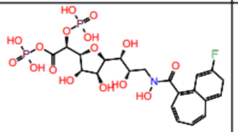 title: P2Y12_HUMAN_1_342_0 : Unreasonable vina: -10. 463	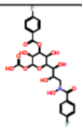 title: P2Y12_HUMAN_1_342_0 : Reasonable vina: -10. 674
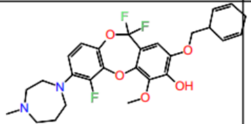 title: SQHC_ALIAD_1_631_0 : Unreasonable vina: -14. 278	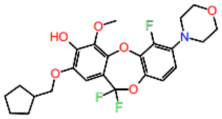 title: SQHC_ALIAD_1_631_0 : Reasonable vina: -17. 408
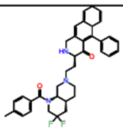 title: BGAT_HUMAN_63_353_0 : Unreasonable vina: -7. 891	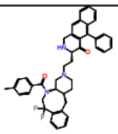 title: BGAT_HUMAN_63_353_0 : Reasonable vina: -9. 201
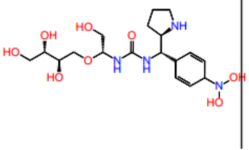 title: CHIB_SERMA_1_499_0 : Unreasonable vina: -7. 115	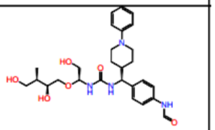 title: CHIB_SERMA_1_499_0 : Reasonable vina: -8. 719

Supporting molecule	CIDD output
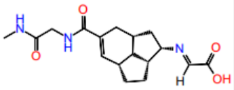 title: BGL07_ORYSJ_25_504_0 : Unreasonable vina: -8. 041	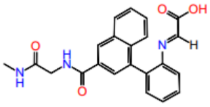 title: BGL07_ORYSJ_25_504_0 : Reasonable vina: -9. 949
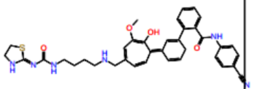 title: TNKS2_HUMAN_948_1162_0 : Unreasonable vina: -10. 284	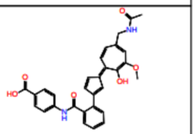 title: TNKS2_HUMAN_948_1162_0 : Reasonable vina: -10. 974
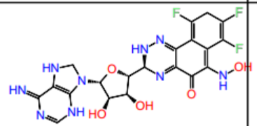 title: HMD_METJA_1_358_0 : Unreasonable vina: -9. 259	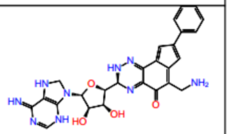 title: HMD_METJA_1_358_0 : Reasonable vina: -10. 458
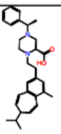 title: SQHC_ALIAD_1_631_0 : Unreasonable vina: -13. 626	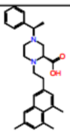 title: SQHC_ALIAD_1_631_0 : Reasonable vina: -13. 825
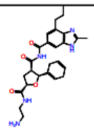 title: CHIB_SERMA_1_499_0 : Unreasonable vina: -10. 676	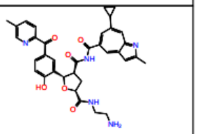 title: CHIB_SERMA_1_499_0 : Reasonable vina: -13. 113
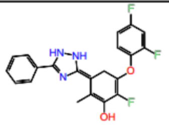 title: NR1H4_HUMAN_258_486_0 : Unreasonable vina: -10. 038	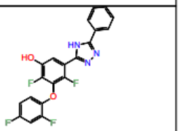 title: NR1H4_HUMAN_258_486_0 : Reasonable vina: -11. 021

Supporting molecule	CIDD output	Supporting molecule	CIDD output
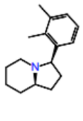 title: SDIA_ECOLI_1_171_0 : Unreasonable vina: -11.019	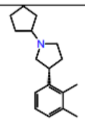 title: SDIA_ECOLI_1_171_0 : Reasonable vina: -11.294	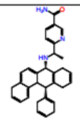 title: SDIA_ECOLI_1_171_0 : Unreasonable vina: -8.52	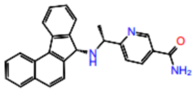 title: SDIA_ECOLI_1_171_0 : Reasonable vina: -13.937
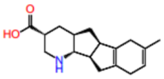 title: GSTP1_HUMAN_2_210_0 : Unreasonable vina: -7.591	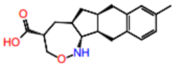 title: GSTP1_HUMAN_2_210_0 : Reasonable vina: -8.725	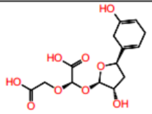 title: HDHA_ECOLI_1_255_0 : Unreasonable vina: -7.709	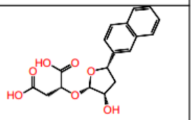 title: HDHA_ECOLI_1_255_0 : Reasonable vina: -8.778
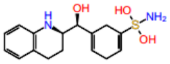 title: HDHA_ECOLI_1_255_0 : Unreasonable vina: -8.5	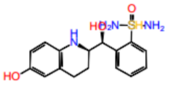 title: HDHA_ECOLI_1_255_0 : Reasonable vina: -8.515	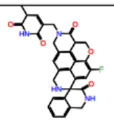 title: NOS1_HUMAN_302_723_0 : Unreasonable vina: -11.943	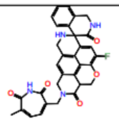 title: NOS1_HUMAN_302_723_0 : Reasonable vina: -12.979
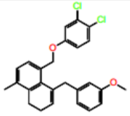 title: IDHP_HUMAN_40_452_0 : Unreasonable vina: -8.176	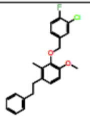 title: IDHP_HUMAN_40_452_0 : Reasonable vina: -10.774	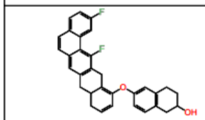 title: NR1H4_HUMAN_258_486_0 : Unreasonable vina: -6.824	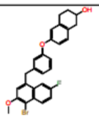 title: NR1H4_HUMAN_258_486_0 : Reasonable vina: -8.578
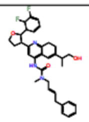 title: IDHP_HUMAN_40_452_0 : Unreasonable vina: -7.605	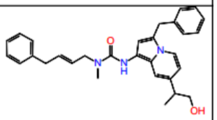 title: IDHP_HUMAN_40_452_0 : Reasonable vina: -11.661	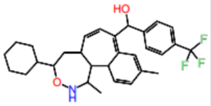 title: CPXB_BACMB_2_464_0 : Unreasonable vina: -9.607	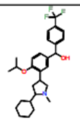 title: CPXB_BACMB_2_464_0 : Reasonable vina: -10.132
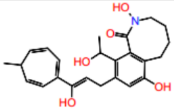 title: AK1BA_HUMAN_1_316_0 : Unreasonable vina: -9.845	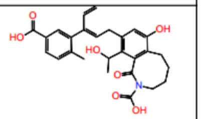 title: AK1BA_HUMAN_1_316_0 : Reasonable vina: -9.981	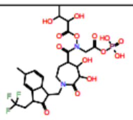 title: P2Y12_HUMAN_1_342_0 : Unreasonable vina: -7.75	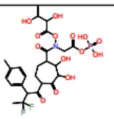 title: P2Y12_HUMAN_1_342_0 : Reasonable vina: -16.253
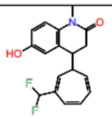 title: OLIAC_CANSA_1_101_0 : Unreasonable vina: -7.631	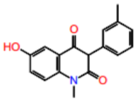 title: OLIAC_CANSA_1_101_0 : Reasonable vina: -8.866	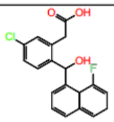 title: SIR3_HUMAN_117_398_0 : Unreasonable vina: -8.238	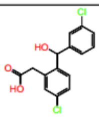 title: SIR3_HUMAN_117_398_0 : Reasonable vina: -8.331

Supporting molecule	CIDD output	Supporting molecule	CIDD output
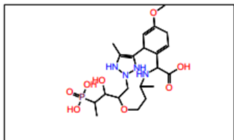 title: MCCF_ECOLX_1_344_0 : Unreasonable vina: -8. 726	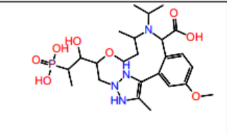 title: MCCF_ECOLX_1_344_0 : Reasonable vina: -8. 947	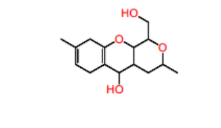 title: DIDH_RAT_1_319_0 : Unreasonable vina: -8. 26	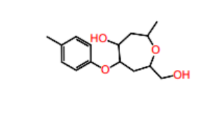 title: DIDH_RAT_1_319_0 : Reasonable vina: -8. 722
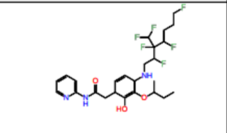 title: IDHP_HUMAN_40_452_0 : Unreasonable vina: -7. 796	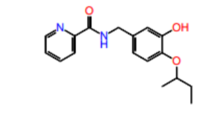 title: IDHP_HUMAN_40_452_0 : Reasonable vina: -11. 383	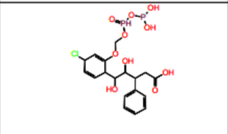 title: COAA_MYCTU_1_312_0 : Unreasonable vina: -7. 572	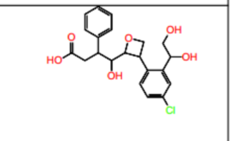 title: COAA_MYCTU_1_312_0 : Reasonable vina: -8. 731
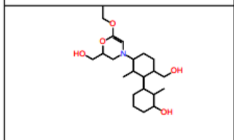 title: AKT1_HUMAN_1_137_0 : Unreasonable vina: -8. 605	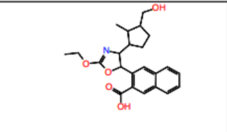 title: AKT1_HUMAN_1_137_0 : Reasonable vina: -9. 926	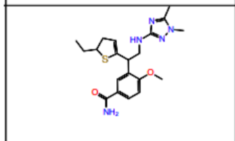 title: M3K14_HUMAN_321_678_0 : Unreasonable vina: -7. 453	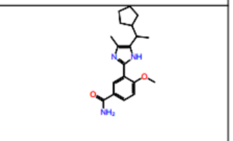 title: M3K14_HUMAN_321_678_0 : Reasonable vina: -9. 209
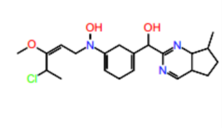 title: HMD_METJA_1_358_0 : Unreasonable vina: -7. 825	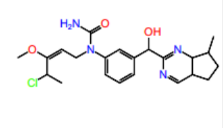 title: HMD_METJA_1_358_0 : Reasonable vina: -8. 55	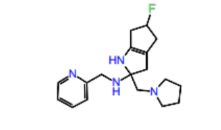 title: CHIB1_ASPFM_39_433_0 : Unreasonable vina: -8. 054	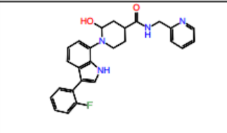 title: CHIB1_ASPFM_39_433_0 : Reasonable vina: -10. 096
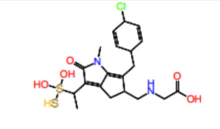 title: SIR3_HUMAN_117_398_0 : Unreasonable vina: -7. 93	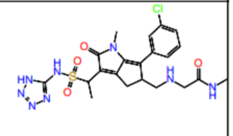 title: SIR3_HUMAN_117_398_0 : Reasonable vina: -10. 435	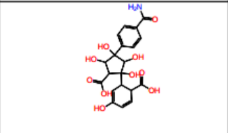 title: SIR3_HUMAN_117_398_0 : Unreasonable vina: -6. 991	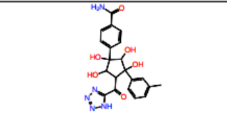 title: SIR3_HUMAN_117_398_0 : Reasonable vina: -10. 758
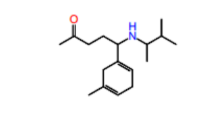 title: DYRK2_HUMAN_145_550_0 : Unreasonable vina: -7. 961	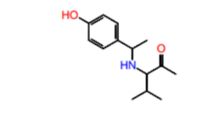 title: DYRK2_HUMAN_145_550_0 : Reasonable vina: -8. 399	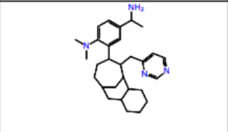 title: NOS3_HUMAN_65_480_0 : Unreasonable vina: -9. 583	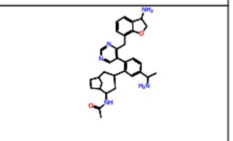 title: NOS3_HUMAN_65_480_0 : Reasonable vina: -10. 652
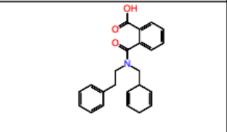 title: DIDH_RAT_1_319_0 : Unreasonable vina: -9. 165	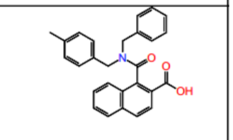 title: DIDH_RAT_1_319_0 : Reasonable vina: -10. 631	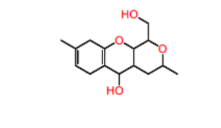 title: DIDH_RAT_1_319_0 : Unreasonable vina: -8. 503	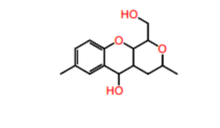 title: DIDH_RAT_1_319_0 : Reasonable vina: -8. 895

Supporting molecule	CIDD output
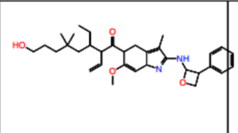 title: BACE2_HUMAN_76_460_0 : Unreasonable vina: -8.586	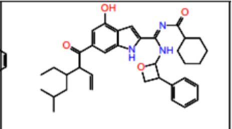 title: BACE2_HUMAN_76_460_0 : Reasonable vina: -9.854
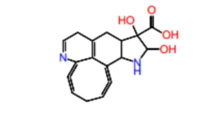 title: F16P1_HUMAN_1_338_0 : Unreasonable vina: -8.173	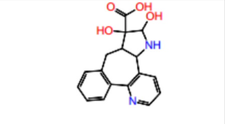 title: F16P1_HUMAN_1_338_0 : Reasonable vina: -8.633
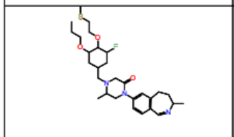 title: CAT_ECOLX_1_219_0 : Unreasonable vina: -9.838	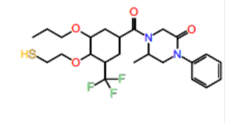 title: CAT_ECOLX_1_219_0 : Reasonable vina: -10.164
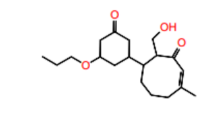 title: DFPA_LOLVU_2_314_0 : Unreasonable vina: -7.208	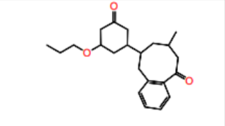 title: DFPA_LOLVU_2_314_0 : Reasonable vina: -8.581
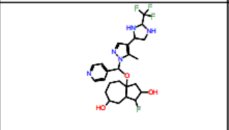 title: QPCT_HUMAN_33_361_0 : Unreasonable vina: -8.178	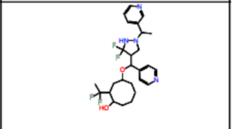 title: QPCT_HUMAN_33_361_0 : Reasonable vina: -9.527
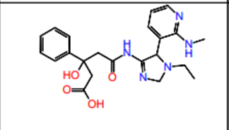 title: KS6A3_HUMAN_41_357_0 : Unreasonable vina: -8.242	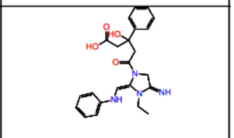 title: KS6A3_HUMAN_41_357_0 : Reasonable vina: -8.738
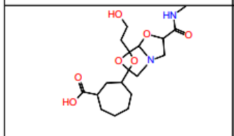 title: AROE_THET8_1_263_0 : Unreasonable vina: -8.741	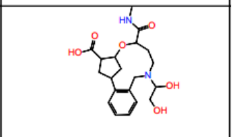 title: AROE_THET8_1_263_0 : Reasonable vina: -8.794

Supporting molecule	CIDD output
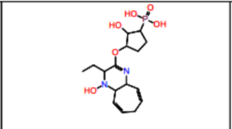 title: GRK4_HUMAN_1_578_0 : Unreasonable vina: -7.158	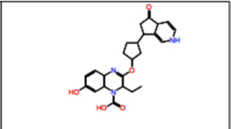 title: GRK4_HUMAN_1_578_0 : Reasonable vina: -8.93
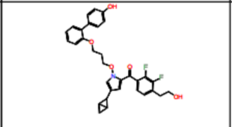 title: CPXB_BACMB_2_464_0 : Unreasonable vina: -10.201	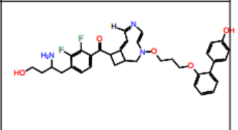 title: CPXB_BACMB_2_464_0 : Reasonable vina: -11.121
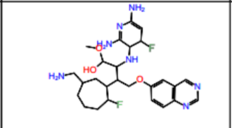 title: BSD_ASPTE_1_130_0 : Unreasonable vina: -7.492	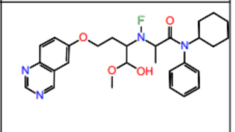 title: BSD_ASPTE_1_130_0 : Reasonable vina: -8.786
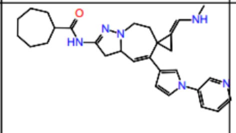 title: RG1_RAUSE_1_513_0 : Unreasonable vina: -10.06	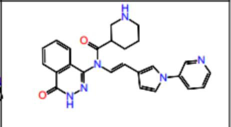 title: RG1_RAUSE_1_513_0 : Reasonable vina: -11.978
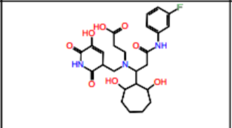 title: QPCT_HUMAN_33_361_0 : Unreasonable vina: -7.531	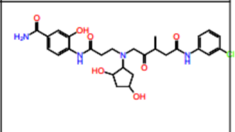 title: QPCT_HUMAN_33_361_0 : Reasonable vina: -8.356
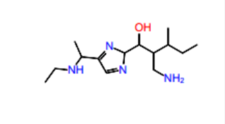 title: GUX1_HYPJE_18_451_0 : Unreasonable vina: -7.25	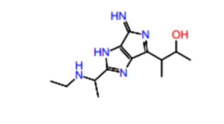 title: GUX1_HYPJE_18_451_0 : Reasonable vina: -8.375
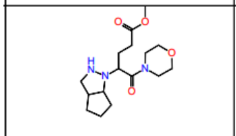 title: UPPS_ECOLI_1_253_0 : Unreasonable vina: -7.288	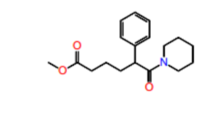 title: UPPS_ECOLI_1_253_0 : Reasonable vina: -8.315

Supporting molecule	CIDD output
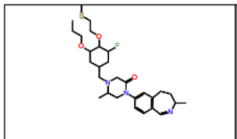 title: CAT_ECOLX_1_219_0 : Unreasonable vina: -9.836	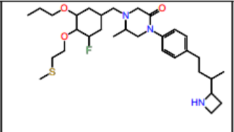 title: CAT_ECOLX_1_219_0 : Reasonable vina: -11.246
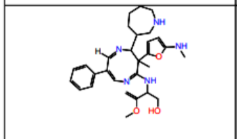 title: NOS2_HUMAN_78_505_0 : Unreasonable vina: -10.504	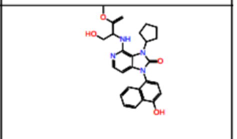 title: NOS2_HUMAN_78_505_0 : Reasonable vina: -11.006
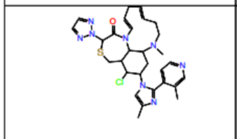 title: BTRN_BACCI_2_250_0 : Unreasonable vina: -4.306	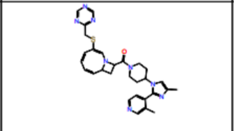 title: BTRN_BACCI_2_250_0 : Reasonable vina: -11.729
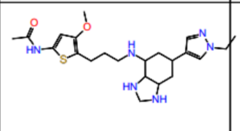 title: ACE_HUMAN_650_1230_0 : Unreasonable vina: -9.498	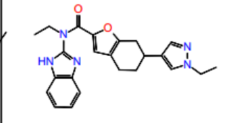 title: ACE_HUMAN_650_1230_0 : Reasonable vina: -10.987
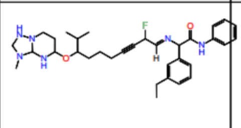 title: AKT1_HUMAN_1_137_0 : Unreasonable vina: -11.185	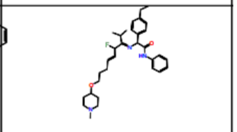 title: AKT1_HUMAN_1_137_0 : Reasonable vina: -11.293
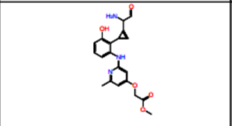 title: BAPA_SPHXN_30_402_0 : Unreasonable vina: -7.681	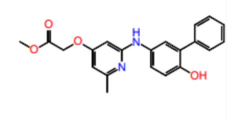 title: BAPA_SPHXN_30_402_0 : Reasonable vina: -8.683

Supporting molecule	CIDD output
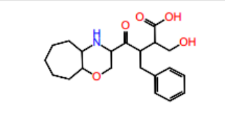 title: ATS5_HUMAN_262_480_0 : Unreasonable vina: -8.133	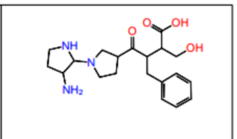 title: ATS5_HUMAN_262_480_0 : Reasonable vina: -8.863
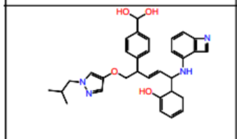 title: NOS2_HUMAN_78_505_0 : Unreasonable vina: -10.76	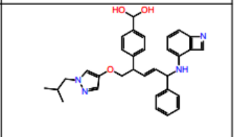 title: NOS2_HUMAN_78_505_0 : Reasonable vina: -12.037
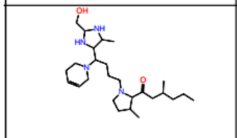 title: ACE_HUMAN_650_1230_0 : Unreasonable vina: -8.564	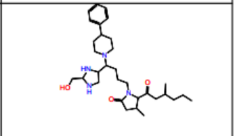 title: ACE_HUMAN_650_1230_0 : Reasonable vina: -10.503
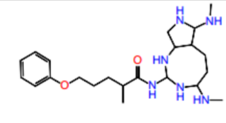 title: ACE_HUMAN_650_1230_0 : Unreasonable vina: -8.69	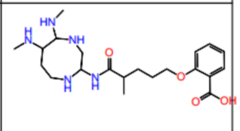 title: ACE_HUMAN_650_1230_0 : Reasonable vina: -8.905
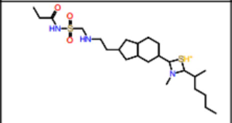 title: TBK1_HUMAN_1_303_0 : Unreasonable vina: -7.693	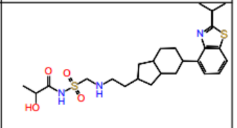 title: TBK1_HUMAN_1_303_0 : Reasonable vina: -8.868
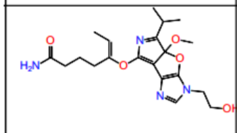 title: BAPA_SPHXN_30_402_0 : Unreasonable vina: -7.794	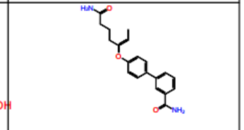 title: BAPA_SPHXN_30_402_0 : Reasonable vina: -8.198

Supporting molecule	CIDD output
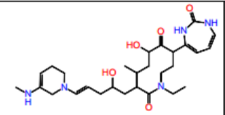 title: PHKG1_RABIT_6_296_ATPsite_0 : Unreasonable vina: -8.922	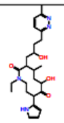 title: PHKG1_RABIT_6_296_ATPsite_0 : Reasonable vina: -9.205
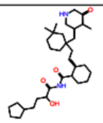 title: RG1_RAUSE_1_513_0 : Unreasonable vina: -10.484	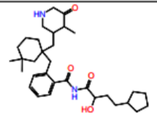 title: RG1_RAUSE_1_513_0 : Reasonable vina: -11.024
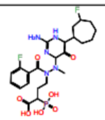 title: CD38_HUMAN_44_300_0 : Unreasonable vina: -8.72	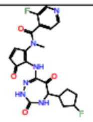 title: CD38_HUMAN_44_300_0 : Reasonable vina: -9.327
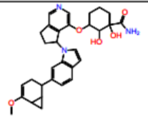 title: XANLY_BACGL_26_777_0 : Unreasonable vina: -9.053	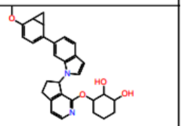 title: XANLY_BACGL_26_777_0 : Reasonable vina: -9.483
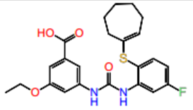 title: PPIA_HUMAN_1_165_0 : Unreasonable vina: -8.023	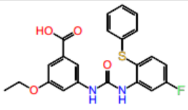 title: PPIA_HUMAN_1_165_0 : Reasonable vina: -8.605
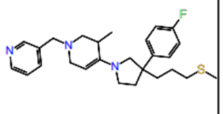 title: SQHC_ALIAD_1_631_0 : Unreasonable vina: -11.51	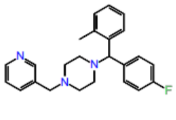 title: SQHC_ALIAD_1_631_0 : Reasonable vina: -14.292

Supporting molecule	CIDD output
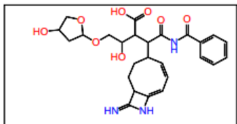 title: BGL07_ORYSJ_25_504_0 : Unreasonable vina: -10.446	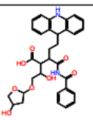 title: BGL07_ORYSJ_25_504_0 : Reasonable vina: -10.592
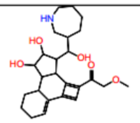 title: DPP2_HUMAN_27_492_0 : Unreasonable vina: -9.855	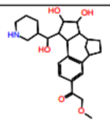 title: DPP2_HUMAN_27_492_0 : Reasonable vina: -11.224
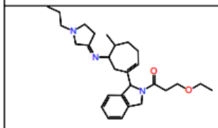 title: PTGIS_HUMAN_20_500_0 : Unreasonable vina: -8.318	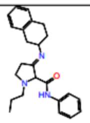 title: PTGIS_HUMAN_20_500_0 : Reasonable vina: -9.448
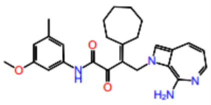 title: PPIA_HUMAN_1_165_0 : Unreasonable vina: -8.777	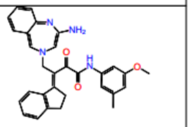 title: PPIA_HUMAN_1_165_0 : Reasonable vina: -10.083
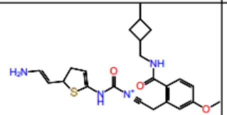 title: HMD_METJA_1_358_0 : Unreasonable vina: -8.349	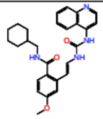 title: HMD_METJA_1_358_0 : Reasonable vina: -9.593
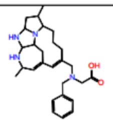 title: KS6A3_HUMAN_41_357_0 : Unreasonable vina: -8.967	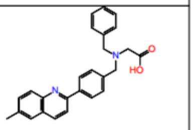 title: KS6A3_HUMAN_41_357_0 : Reasonable vina: -11.101

Supporting molecule	CIDD output	Supporting molecule	CIDD output
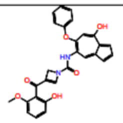 title: KS6A3_HUMAN_41_357_0 : Unreasonable vina: -9.414	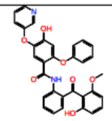 title: KS6A3_HUMAN_41_357_0 : Reasonable vina: -9.746	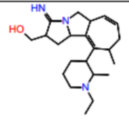 title: DYRK2_HUMAN_145_550_0 : Unreasonable vina: -6.725	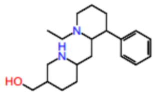 title: DYRK2_HUMAN_145_550_0 : Reasonable vina: -9.337
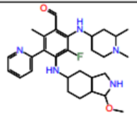 title: NR1H4_HUMAN_258_486_0 : Unreasonable vina: -3.528	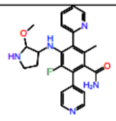 title: NR1H4_HUMAN_258_486_0 : Reasonable vina: -14.043	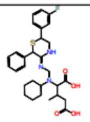 title: BACE2_HUMAN_76_460_0 : Unreasonable vina: -9.145	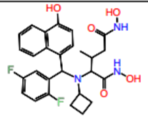 title: BACE2_HUMAN_76_460_0 : Reasonable vina: -9.806
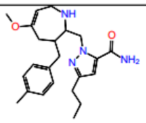 title: SDIA_ECOLI_1_171_0 : Unreasonable vina: -10.997	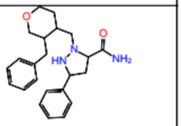 title: SDIA_ECOLI_1_171_0 : Reasonable vina: -13.15	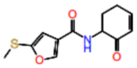 title: TRAR_RHIRD_1_234_0 : Unreasonable vina: -8.935	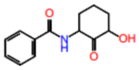 title: TRAR_RHIRD_1_234_0 : Reasonable vina: -12.018
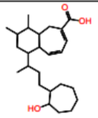 title: HDHA_ECOLI_1_255_0 : Unreasonable vina: -9.845	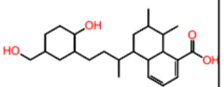 title: HDHA_ECOLI_1_255_0 : Reasonable vina: -9.957	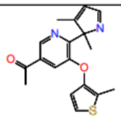 title: UPPS_ECOLI_1_253_0 : Unreasonable vina: -7.717	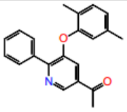 title: UPPS_ECOLI_1_253_0 : Reasonable vina: -10.031
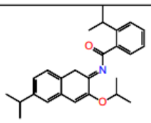 title: IDHP_HUMAN_40_452_0 : Unreasonable vina: -8.034	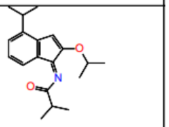 title: IDHP_HUMAN_40_452_0 : Reasonable vina: -10.368	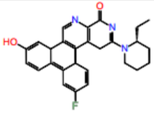 title: ABL2_HUMAN_274_551_0 : Unreasonable vina: -10.488	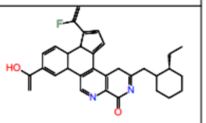 title: ABL2_HUMAN_274_551_0 : Reasonable vina: -10.776
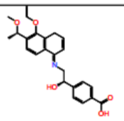 title: AKT1_HUMAN_1_137_0 : Unreasonable vina: -10.124	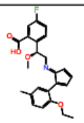 title: AKT1_HUMAN_1_137_0 : Reasonable vina: -10.13	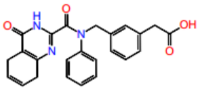 title: : Unreasonable vina: -10.487	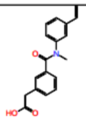 title: : Reasonable vina: -10.893

Supporting molecule	CIDD output	Supporting molecule	CIDD output
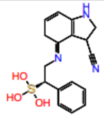 title: MURA_ECOLI_1_419_catalytic_0 : Unreasonable vina: -8.295	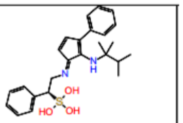 title: MURA_ECOLI_1_419_catalytic_0 : Reasonable vina: -9.241	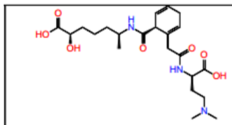 title: BGL07_ORYSJ_25_504_0 : Unreasonable vina: -8.187	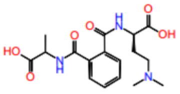 title: BGL07_ORYSJ_25_504_0 : Reasonable vina: -8.434
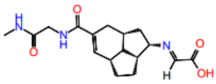 title: BGL07_ORYSJ_25_504_0 : Unreasonable vina: -8.028	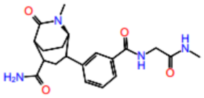 title: BGL07_ORYSJ_25_504_0 : Reasonable vina: -9.632	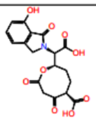 title: PAC_ECOLX_27_846_0 : Unreasonable vina: -8.228	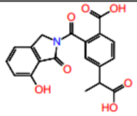 title: PAC_ECOLX_27_846_0 : Reasonable vina: -8.313
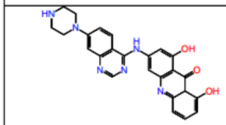 title: PAC_ECOLX_27_846_0 : Unreasonable vina: -9.538	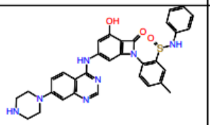 title: PAC_ECOLX_27_846_0 : Reasonable vina: -10.042	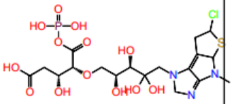 title: P2Y12_HUMAN_1_342_0 : Unreasonable vina: -8.514	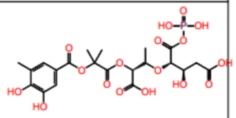 title: P2Y12_HUMAN_1_342_0 : Reasonable vina: -8.942
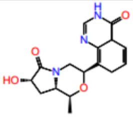 title: EXG1_CANAL_41_438_0 : Unreasonable vina: -9.965	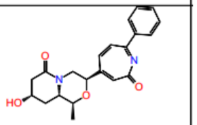 title: EXG1_CANAL_41_438_0 : Reasonable vina: -10.569	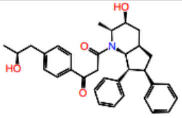 title: FKB1A_HUMAN_2_108_0 : Unreasonable vina: -7.899	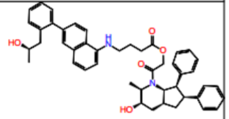 title: FKB1A_HUMAN_2_108_0 : Reasonable vina: -8.786
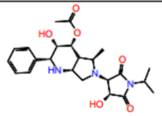 title: CHIB_SERMA_1_499_0 : Unreasonable vina: -9.972	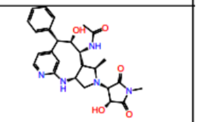 title: CHIB_SERMA_1_499_0 : Reasonable vina: -10.354	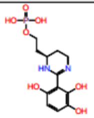 title: KS6A3_HUMAN_41_357_0 : Unreasonable vina: -7.827	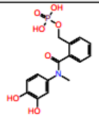 title: KS6A3_HUMAN_41_357_0 : Reasonable vina: -8.545
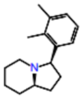 title: SDIA_ECOLI_1_171_0 : Unreasonable vina: -10.933	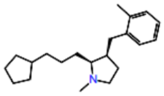 title: SDIA_ECOLI_1_171_0 : Reasonable vina: -11.339	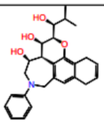 title: GUX1_HYPJE_18_451_0 : Unreasonable vina: -10.767	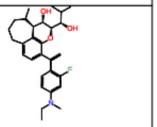 title: GUX1_HYPJE_18_451_0 : Reasonable vina: -12.3

Supporting molecule	CIDD output	Supporting molecule	CIDD output
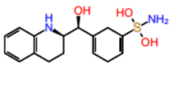 title: HDHA_ECOLI_1_255_0 : Unreasonable vina: -8.511	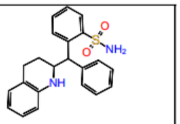 title: HDHA_ECOLI_1_255_0 : Reasonable vina: -9.995	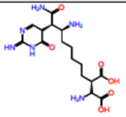 title: ODBB_THET8_1_324_0 : Unreasonable vina: -9.002	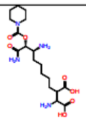 title: ODBB_THET8_1_324_0 : Reasonable vina: -9.322
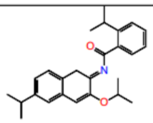 title: IDHP_HUMAN_40_452_0 : Unreasonable vina: -8.039	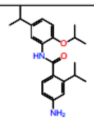 title: IDHP_HUMAN_40_452_0 : Reasonable vina: -9.819	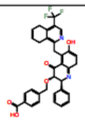 title: CPXB_BACMB_2_464_0 : Unreasonable vina: -9.196	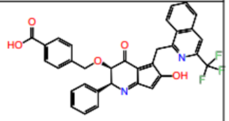 title: CPXB_BACMB_2_464_0 : Reasonable vina: -12.034
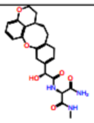 title: NOS1_HUMAN_302_723_0 : Unreasonable vina: -9.495	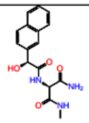 title: NOS1_HUMAN_302_723_0 : Reasonable vina: -9.579	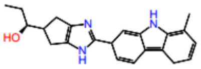 title: NOS1_HUMAN_302_723_0 : Unreasonable vina: -10.062	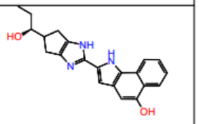 title: NOS1_HUMAN_302_723_0 : Reasonable vina: -10.305
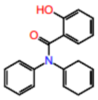 title: CAT_ECOLX_1_219_0 : Unreasonable vina: -9.2	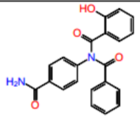 title: CAT_ECOLX_1_219_0 : Reasonable vina: -13.057	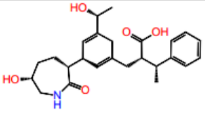 title: BSD_ASPTE_1_130_0 : Unreasonable vina: -8.807	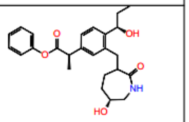 title: BSD_ASPTE_1_130_0 : Reasonable vina: -9.501
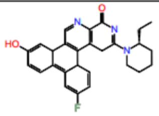 title: ABL2_HUMAN_274_551_0 : Unreasonable vina: -10.702	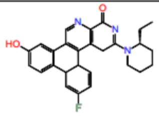 title: ABL2_HUMAN_274_551_0 : Reasonable vina: -11.583	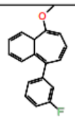 title: NQO1_HUMAN_2_274_0 : Unreasonable vina: -9.262	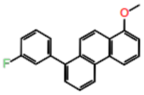 title: NQO1_HUMAN_2_274_0 : Reasonable vina: -10.424
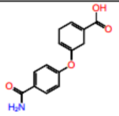 title: BTRN_BACCI_2_250_0 : Unreasonable vina: -8.786	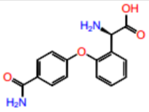 title: BTRN_BACCI_2_250_0 : Reasonable vina: -8.951	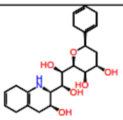 title: NAGZ_VIBCH_1_330_0 : Unreasonable vina: -7.206	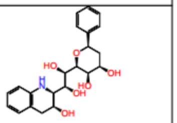 title: NAGZ_VIBCH_1_330_0 : Reasonable vina: -8.307
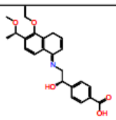 title: AKT1_HUMAN_1_137_0 : Unreasonable vina: -10.1	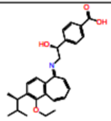 title: AKT1_HUMAN_1_137_0 : Reasonable vina: -11.478	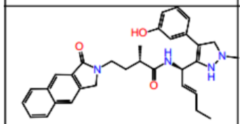 title: AKT1_HUMAN_1_137_0 : Unreasonable vina: -12.405	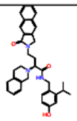 title: AKT1_HUMAN_1_137_0 : Reasonable vina: -13.048

Supporting molecule	CIDD output	Supporting molecule	CIDD output
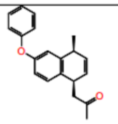 title: PA21B_PIG_23_146_0 : Unreasonable vina: -8.391	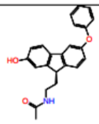 title: PA21B_PIG_23_146_0 : Reasonable vina: -10.029	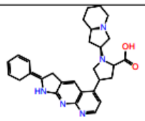 title: PHKG1_RABIT_6_296_ATPsite_0 : Unreasonable vina: -10.937	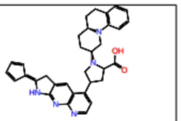 title: PHKG1_RABIT_6_296_ATPsite_0 : Reasonable vina: -13.466
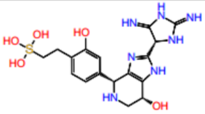 title: M3K14_HUMAN_321_678_0 : Unreasonable vina: -8.948	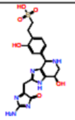 title: M3K14_HUMAN_321_678_0 : Reasonable vina: -9.001	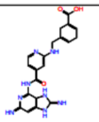 title: M3K14_HUMAN_321_678_0 : Unreasonable vina: -9.44	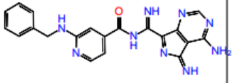 title: M3K14_HUMAN_321_678_0 : Reasonable vina: -9.899
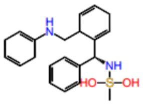 title: PTGIS_HUMAN_20_500_0 : Unreasonable vina: -7.955	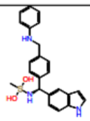 title: PTGIS_HUMAN_20_500_0 : Reasonable vina: -9.193	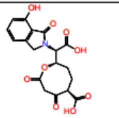 title: PAC_ECOLX_27_846_0 : Unreasonable vina: -7.907	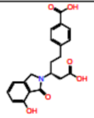 title: PAC_ECOLX_27_846_0 : Reasonable vina: -8.704
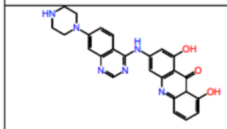 title: PAC_ECOLX_27_846_0 : Unreasonable vina: -9.272	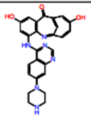 title: PAC_ECOLX_27_846_0 : Reasonable vina: -9.421	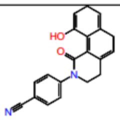 title: TNKS2_HUMAN_948_1162_0 : Unreasonable vina: -10.215	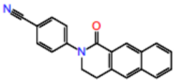 title: TNKS2_HUMAN_948_1162_0 : Reasonable vina: -12.537
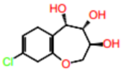 title: XANLY_BACGL_26_777_0 : Unreasonable vina: -6.991	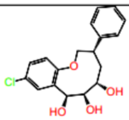 title: XANLY_BACGL_26_777_0 : Reasonable vina: -8.994	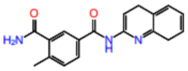 title: PPIA_HUMAN_1_165_0 : Unreasonable vina: -9.243	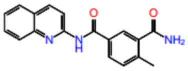 title: PPIA_HUMAN_1_165_0 : Reasonable vina: -9.435
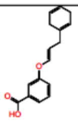 title: PPIA_HUMAN_1_165_0 : Unreasonable vina: -7.765	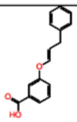 title: PPIA_HUMAN_1_165_0 : Reasonable vina: -8.447	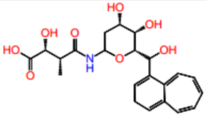 title: P2Y12_HUMAN_1_342_0 : Unreasonable vina: -8.744	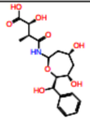 title: P2Y12_HUMAN_1_342_0 : Reasonable vina: -10.352

Supporting molecule	CIDD output	Supporting molecule	CIDD output
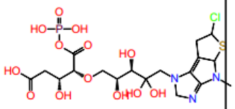 title: P2Y12_HUMAN_1_342_0 : Unreasonable vina: -8.31	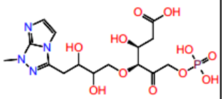 title: P2Y12_HUMAN_1_342_0 : Reasonable vina: -9.509	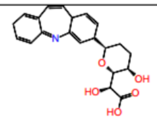 title: EXG1_CANAL_41_438_0 : Unreasonable vina: -10.072	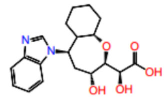 title: EXG1_CANAL_41_438_0 : Reasonable vina: -10.17
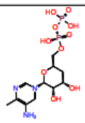 title: MENE_BACSU_2_486_0 : Unreasonable vina: -8.029	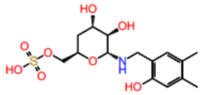 title: MENE_BACSU_2_486_0 : Reasonable vina: -8.629	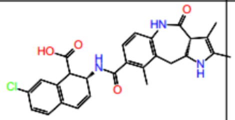 title: SQHC_ALIAD_1_631_0 : Unreasonable vina: -9.519	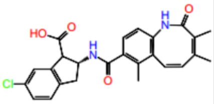 title: SQHC_ALIAD_1_631_0 : Reasonable vina: -12.291
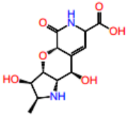 title: CHIB_SERMA_1_499_0 : Unreasonable vina: -7.389	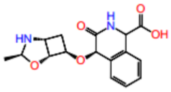 title: CHIB_SERMA_1_499_0 : Reasonable vina: -9.388	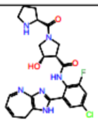 title: SIR3_HUMAN_117_398_0 : Unreasonable vina: -10.258	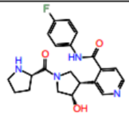 title: SIR3_HUMAN_117_398_0 : Reasonable vina: -10.419
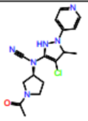 title: DYRK2_HUMAN_145_550_0 : Unreasonable vina: -7.898	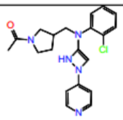 title: DYRK2_HUMAN_145_550_0 : Reasonable vina: -9.098	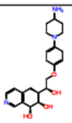 title: NOS3_HUMAN_65_480_0 : Unreasonable vina: -9.821	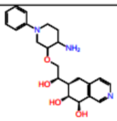 title: NOS3_HUMAN_65_480_0 : Reasonable vina: -10.535
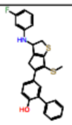 title: NR1H4_HUMAN_258_486_0 : Unreasonable vina: -8.974	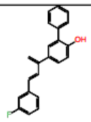 title: NR1H4_HUMAN_258_486_0 : Reasonable vina: -9.969	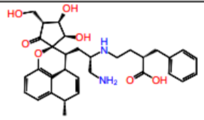 title: BACE2_HUMAN_76_460_0 : Unreasonable vina: -9.302	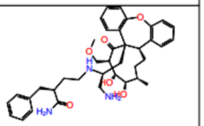 title: BACE2_HUMAN_76_460_0 : Reasonable vina: -9.947
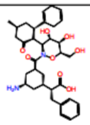 title: BACE2_HUMAN_76_460_0 : Unreasonable vina: -9.473	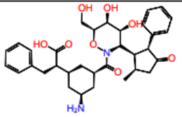 title: BACE2_HUMAN_76_460_0 : Reasonable vina: -9.828	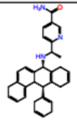 title: SDIA_ECOLI_1_171_0 : Unreasonable vina: -8.889	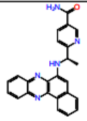 title: SDIA_ECOLI_1_171_0 : Reasonable vina: -13.779
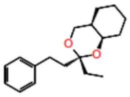 title: TRAR_RHIRD_1_234_0 : Unreasonable vina: -10.182	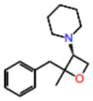 title: TRAR_RHIRD_1_234_0 : Reasonable vina: -13.112	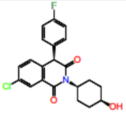 title: TRAR_RHIRD_1_234_0 : Unreasonable vina: -9.69	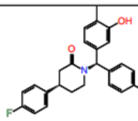 title: TRAR_RHIRD_1_234_0 : Reasonable vina: -15.856

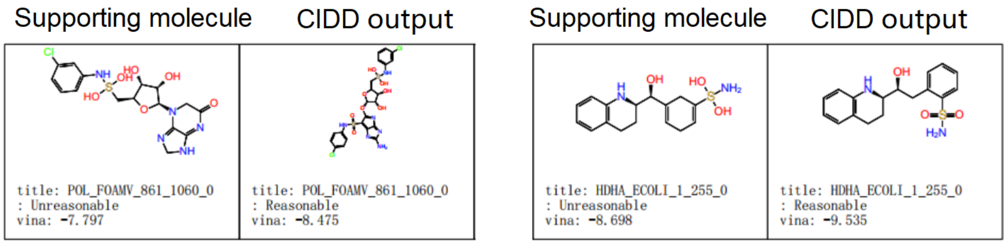

I Limitation on Computational Cost and Scalability

We acknowledge that our framework introduces additional computational steps due to the use of LLM-based modules. Below, we provide a detailed discussion of the computational overhead, empirical runtime, and justification for its practicality in the context of drug discovery.

Computational Overhead of LLM Pipelines. The runtime and token-related costs associated with repeated LLM invocations—such as scaffold analysis, molecule generation, self-reflection, and candidate selection—can introduce non-trivial computational overhead. However, several factors mitigate this concern:

LLM Inference Efficiency Is Rapidly Improving. Recent advances in model quantization, prompt batching, and optimized inference are dramatically reducing the cost of multi-step reasoning. For example, DeepSeek-V3/R1 achieves approximately 2.19M output tokens per dollar, reflecting a 60–70% cost reduction compared to GPT-4 in 2023. Frameworks such as `vLLM` [18], `vTensor` [36], and `Splitwiser` [1] further improve efficiency: `vLLM` enables up to 24× throughput; `vTensor` achieves 2× speedups with 70% less GPU memory; and `Splitwiser` reduces latency by 1.7× through prompt colocation. Hardware accelerators like TensorRT-LLM also support highly scalable domain-specific pipelines. These trends suggest that the cost of multi-step reasoning is unlikely to remain a long-term bottleneck.

Empirical Runtime of Our Pipeline. To provide a more quantitative view, we report the empirical runtime of our full pipeline. Based on our experiments with the `MolCraft` model (used as the SBIG module in our method), under the setting of 100 sampling steps, it takes approximately 300 seconds to generate 100 molecules. For competitive baselines, previous work reports that the autoregressive method `Pocket2Mol` requires around 2827 seconds to generate the same number of molecules, and diffusion-based methods such as `TargetDiff` and `DecompDiff` require approximately 3428 seconds and 6189 seconds, respectively.

As our method builds upon base SBDD models as the SBIG module, we only consider the additional time introduced by the LEDD module. With parallel LLM API requests, the total time required for generating 100 molecules is approximately 15 minutes in our experiments. Importantly, this added cost does not change the order of magnitude of the overall runtime.

The majority of this overhead stems from LLM inference latency, which is common across recent works that utilize LLMs. Nevertheless, this is unlikely to remain a bottleneck as inference efficiency continues to improve. For instance, recent advances in Diffusion-LLMs [31] have demonstrated inference speeds exceeding 2000 tokens per second, suggesting the potential for up to a 20× acceleration of our pipeline in the near future.

Molecule Design Is Not a Real-Time Task. Unlike latency-sensitive domains such as recommendation systems or autonomous control, molecule design prioritizes quality over speed. Drug discovery workflows are inherently iterative and require careful validation. While LLM-agent pipelines incur additional compute, their ability to generate higher-quality candidates with stronger binding plausibility aligns with the broader goal of improving experimental success rates, rather than immediate response times.

Relative Cost Compared to Wet-Lab Validation. In the broader context of drug development—which routinely spans several years and billions of dollars—LLM-related inference costs are marginal. The true bottlenecks lie in experimental synthesis, biochemical testing, and preclinical validation. Even modest improvements in in silico candidate quality can translate to significant downstream savings. Thus, the human-effort and resource reductions enabled by automated multi-step reasoning justify the modest computational overhead.

In summary, while our method introduces additional computational cost, it remains within a practical and acceptable range and does not diminish the significance, effectiveness, or applicability of our contributions. These tradeoffs will continue to improve as inference efficiency advances.

J Results on more targets

we tested CIDD on additional targets: 1sa1, 1t8i and 7rpz, all known for their structural complexity and variability in ligand scaffolds. For 1sa1, Tubulin presents a challenging drug target because its binding sites are highly dynamic, involving extensive protein–protein interfaces; furthermore, the ligand in this complex, podophyllotoxin, is a complex natural product scaffold[28]. For 1t8i, Human DNA Topoisomerase I presents a challenging drug target because its catalytic mechanism involves a highly dynamic binding site that accommodates DNA; moreover, the ligand in this initial complex is camptothecin, a natural product scaffold rather than a traditionally rationally designed small molecule[32]. For 7rpz, KRASG12D is difficult to inhibit due to its high GDP/GTP affinity and absence of a nucleophilic residue near the switch II pocket, which hampers covalent strategies and limits prior chemotypes. The ligand uniquely overcomes these barriers with a pyrido[4,3-d]pyrimidine scaffold, fully engages the pocket, and achieves picomolar noncovalent inhibition with strong in vivo efficacy[35].

Table 5: Comparison between MolCRAFT and CIDD on different targets

Target	Method	Success Ratio ↑	Vina Score ↓	QED ↑	SA ↑	MRR ↑
1sa1	MolCRAFT	27.78%	-9.78	0.56	0.66	35.56%
1sa1	CIDD	54.44%	-10.47	0.60	0.71	62.22%
1t8i	MolCRAFT	9.64%	-7.96	0.37	0.57	60.24%
1t8i	CIDD	27.71%	-8.38	0.39	0.62	68.67%
7rpz	MolCRAFT	1.35%	-9.71	0.27	0.57	1.35%
7rpz	CIDD	14.86%	-10.35	0.32	0.61	14.86%

K Ablation Study: Reasoning Design vs. Simple Prompting

To investigate the source of our framework's effectiveness, we conducted an ablation study comparing different prompting strategies. Specifically, we replaced our original chain-of-thought (CoT), domain-informed prompt with a simplified instruction: *"Based on the pocket and interaction analysis, modify the original molecule."*

This experiment isolates the effect of prompt engineering by using the same underlying LLM and tools, but with varying reasoning structure.

Table 6: Ablation results comparing the impact of prompt complexity on model performance.

Method	SA ↑	MRR ↑	Success ↑
MolCRAFT (baseline)	0.685	58.47%	13.72%
CIDD (simple prompt)	0.678	63.69%	19.76%
CIDD (CoT prompt, ours)	0.735	81.74%	34.59%

Despite using the same LLM and external tools, the simplified prompting strategy performs significantly worse than our CoT-guided approach, and only marginally better than the MolCRAFT baseline. This highlights that the primary gains of our method stem from structured, domain-informed reasoning embedded in the prompt design, rather than from tool integration alone.

L Extension: Applicability to Hit-to-Lead Optimization

While the CIDD framework was not originally designed for hit-to-lead optimization, it can be readily adapted to such scenarios. To explore this possibility, we initialized the generation process—and the input to the LEDD module—using ground-truth ligands from the CrossDocked test set.

Despite these ligands already demonstrating strong synthetic accessibility and structural quality, CIDD was able to generate new molecules that exhibited further improvements in potency (as measured by docking score), synthesizability (QED and SA), and overall reasonability (MRR and success ratio).

Table 7: Evaluation of hit-to-lead potential by initializing CIDD with known binders from the CrossDocked test set.

Method	**Vina Score ↓**	**QED ↑**	**SA ↑**	**MRR ↑**	**Success Ratio ↑**
Original Ligands	-7.53	0.473	0.738	0.8272	22.22%
CIDD (generated)	-8.22	0.528	0.752	0.9136	37.04%

These results demonstrate that, even when starting from already high-quality ligands, our framework is capable of discovering improved candidates through domain-aware multi-agent reasoning.

We note that fully supporting hit-to-lead tasks would require adapting the pipeline structure, modifying the chain-of-thought prompts, and refining the integration of design tools to better align with lead optimization objectives. Nonetheless, the observed performance underscores the broader applicability of our framework and the potential of structured LLM reasoning in more advanced drug development stages.

We plan to incorporate support for hit-to-lead optimization more formally in future work.

M Effect of Re-Docking SBIG-Generated Molecules

To ensure molecular stability and structural correctness, our pipeline includes a re-docking step following initial molecule generation. The rationale behind this design choice is that conformations directly produced by generative models may suffer from issues such as atomic clashes or physically unstable geometries, which can negatively affect downstream interaction analysis and overall pipeline reliability. This concern has also been discussed in recent work [**?**]. Re-docking provides a more stable and physically reasonable starting point for the LEDD module.

To evaluate whether this re-docking step is necessary, we conducted an ablation study comparing the performance of our pipeline with and without re-docking. Specifically, we initialized the LEDD module with either (1) re-docked poses or (2) the original generated conformations. All experiments used DeepSeek-V3 as the LLM.

Table 8: Ablation study evaluating the effect of re-docking versus directly using generated conformations.

Method	**Vina Score ↓**	**QED ↑**	**SA ↑**	**MRR ↑**	**Success Ratio ↑**
Re-docking	-8.49	0.565	0.714	76.00%	29.66%
Original conformation	-8.403	0.575	0.721	76.09%	28.03%

As shown in the table, both variants achieve comparable results, with re-docking offering slight improvements in docking score and success ratio, while direct usage of the original conformation shows marginally better QED and SA. Overall, this suggests that our framework is robust to this design decision.

While re-docking provides additional geometric stability, the small performance gap indicates that either choice is acceptable in practice, depending on computational tradeoffs. This flexibility may be useful in settings where runtime is more constrained. .

NeurIPS Paper Checklist

1. **Claims**

   Question: Do the main claims made in the abstract and introduction accurately reflect the paper's contributions and scope?

   Answer: [Yes]

   Justification: The main claims made in the abstract and introduction accurately reflect the paper's contributions and scope.

   Guidelines:

   - The answer NA means that the abstract and introduction do not include the claims made in the paper.
   - The abstract and/or introduction should clearly state the claims made, including the contributions made in the paper and important assumptions and limitations. A No or NA answer to this question will not be perceived well by the reviewers.
   - The claims made should match theoretical and experimental results, and reflect how much the results can be expected to generalize to other settings.
   - It is fine to include aspirational goals as motivation as long as it is clear that these goals are not attained by the paper.

2. **Limitations**

   Question: Does the paper discuss the limitations of the work performed by the authors?

   Answer: [Yes]

   Justification: Limitations are described in the appendix.

   Guidelines:

   - The answer NA means that the paper has no limitation while the answer No means that the paper has limitations, but those are not discussed in the paper.
   - The authors are encouraged to create a separate "Limitations" section in their paper.
   - The paper should point out any strong assumptions and how robust the results are to violations of these assumptions (e.g., independence assumptions, noiseless settings, model well-specification, asymptotic approximations only holding locally). The authors should reflect on how these assumptions might be violated in practice and what the implications would be.
   - The authors should reflect on the scope of the claims made, e.g., if the approach was only tested on a few datasets or with a few runs. In general, empirical results often depend on implicit assumptions, which should be articulated.
   - The authors should reflect on the factors that influence the performance of the approach. For example, a facial recognition algorithm may perform poorly when image resolution is low or images are taken in low lighting. Or a speech-to-text system might not be used reliably to provide closed captions for online lectures because it fails to handle technical jargon.
   - The authors should discuss the computational efficiency of the proposed algorithms and how they scale with dataset size.
   - If applicable, the authors should discuss possible limitations of their approach to address problems of privacy and fairness.
   - While the authors might fear that complete honesty about limitations might be used by reviewers as grounds for rejection, a worse outcome might be that reviewers discover limitations that aren't acknowledged in the paper. The authors should use their best judgment and recognize that individual actions in favor of transparency play an important role in developing norms that preserve the integrity of the community. Reviewers will be specifically instructed to not penalize honesty concerning limitations.

3. **Theory assumptions and proofs**

   Question: For each theoretical result, does the paper provide the full set of assumptions and a complete (and correct) proof?

   Answer: [NA]

Justification: Our paper does not include theoretical results.

Guidelines:

- The answer NA means that the paper does not include theoretical results.
- All the theorems, formulas, and proofs in the paper should be numbered and cross-referenced.
- All assumptions should be clearly stated or referenced in the statement of any theorems.
- The proofs can either appear in the main paper or the supplemental material, but if they appear in the supplemental material, the authors are encouraged to provide a short proof sketch to provide intuition.
- Inversely, any informal proof provided in the core of the paper should be complemented by formal proofs provided in appendix or supplemental material.
- Theorems and Lemmas that the proof relies upon should be properly referenced.

4. **Experimental result reproducibility**

   Question: Does the paper fully disclose all the information needed to reproduce the main experimental results of the paper to the extent that it affects the main claims and/or conclusions of the paper (regardless of whether the code and data are provided or not)?

   Answer: [Yes]

   Justification: We describe the information in the experiment setting section.

   Guidelines:

   - The answer NA means that the paper does not include experiments.
   - If the paper includes experiments, a No answer to this question will not be perceived well by the reviewers: Making the paper reproducible is important, regardless of whether the code and data are provided or not.
   - If the contribution is a dataset and/or model, the authors should describe the steps taken to make their results reproducible or verifiable.
   - Depending on the contribution, reproducibility can be accomplished in various ways. For example, if the contribution is a novel architecture, describing the architecture fully might suffice, or if the contribution is a specific model and empirical evaluation, it may be necessary to either make it possible for others to replicate the model with the same dataset, or provide access to the model. In general. releasing code and data is often one good way to accomplish this, but reproducibility can also be provided via detailed instructions for how to replicate the results, access to a hosted model (e.g., in the case of a large language model), releasing of a model checkpoint, or other means that are appropriate to the research performed.
   - While NeurIPS does not require releasing code, the conference does require all submissions to provide some reasonable avenue for reproducibility, which may depend on the nature of the contribution. For example
     (a) If the contribution is primarily a new algorithm, the paper should make it clear how to reproduce that algorithm.
     (b) If the contribution is primarily a new model architecture, the paper should describe the architecture clearly and fully.
     (c) If the contribution is a new model (e.g., a large language model), then there should either be a way to access this model for reproducing the results or a way to reproduce the model (e.g., with an open-source dataset or instructions for how to construct the dataset).
     (d) We recognize that reproducibility may be tricky in some cases, in which case authors are welcome to describe the particular way they provide for reproducibility. In the case of closed-source models, it may be that access to the model is limited in some way (e.g., to registered users), but it should be possible for other researchers to have some path to reproducing or verifying the results.

5. **Open access to data and code**

   Question: Does the paper provide open access to the data and code, with sufficient instructions to faithfully reproduce the main experimental results, as described in supplemental material?

Answer: [No]

Justification: Codes will be released once the paper is accepted.

Guidelines:

- The answer NA means that paper does not include experiments requiring code.
- Please see the NeurIPS code and data submission guidelines (`https://nips.cc/public/guides/CodeSubmissionPolicy`) for more details.
- While we encourage the release of code and data, we understand that this might not be possible, so "No" is an acceptable answer. Papers cannot be rejected simply for not including code, unless this is central to the contribution (e.g., for a new open-source benchmark).
- The instructions should contain the exact command and environment needed to run to reproduce the results. See the NeurIPS code and data submission guidelines (`https://nips.cc/public/guides/CodeSubmissionPolicy`) for more details.
- The authors should provide instructions on data access and preparation, including how to access the raw data, preprocessed data, intermediate data, and generated data, etc.
- The authors should provide scripts to reproduce all experimental results for the new proposed method and baselines. If only a subset of experiments are reproducible, they should state which ones are omitted from the script and why.
- At submission time, to preserve anonymity, the authors should release anonymized versions (if applicable).
- Providing as much information as possible in supplemental material (appended to the paper) is recommended, but including URLs to data and code is permitted.

6. **Experimental setting/details**

   Question: Does the paper specify all the training and test details (e.g., data splits, hyperparameters, how they were chosen, type of optimizer, etc.) necessary to understand the results?

   Answer: [Yes]

   Justification: We describe the details in the experiment setting section.

   Guidelines:

   - The answer NA means that the paper does not include experiments.
   - The experimental setting should be presented in the core of the paper to a level of detail that is necessary to appreciate the results and make sense of them.
   - The full details can be provided either with the code, in appendix, or as supplemental material.

7. **Experiment statistical significance**

   Question: Does the paper report error bars suitably and correctly defined or other appropriate information about the statistical significance of the experiments?

   Answer: [No]

   Justification: The baseline methods do not have error bars reported.

   Guidelines:

   - The answer NA means that the paper does not include experiments.
   - The authors should answer "Yes" if the results are accompanied by error bars, confidence intervals, or statistical significance tests, at least for the experiments that support the main claims of the paper.
   - The factors of variability that the error bars are capturing should be clearly stated (for example, train/test split, initialization, random drawing of some parameter, or overall run with given experimental conditions).
   - The method for calculating the error bars should be explained (closed form formula, call to a library function, bootstrap, etc.)
   - The assumptions made should be given (e.g., Normally distributed errors).
   - It should be clear whether the error bar is the standard deviation or the standard error of the mean.

- It is OK to report 1-sigma error bars, but one should state it. The authors should preferably report a 2-sigma error bar than state that they have a 96% CI, if the hypothesis of Normality of errors is not verified.
- For asymmetric distributions, the authors should be careful not to show in tables or figures symmetric error bars that would yield results that are out of range (e.g. negative error rates).
- If error bars are reported in tables or plots, The authors should explain in the text how they were calculated and reference the corresponding figures or tables in the text.

8. **Experiments compute resources**

   Question: For each experiment, does the paper provide sufficient information on the computer resources (type of compute workers, memory, time of execution) needed to reproduce the experiments?

   Answer: [Yes]

   Justification: We provide the information in supplementary material.

   Guidelines:

   - The answer NA means that the paper does not include experiments.
   - The paper should indicate the type of compute workers CPU or GPU, internal cluster, or cloud provider, including relevant memory and storage.
   - The paper should provide the amount of compute required for each of the individual experimental runs as well as estimate the total compute.
   - The paper should disclose whether the full research project required more compute than the experiments reported in the paper (e.g., preliminary or failed experiments that didn't make it into the paper).

9. **Code of ethics**

   Question: Does the research conducted in the paper conform, in every respect, with the NeurIPS Code of Ethics `https://neurips.cc/public/EthicsGuidelines`?

   Answer: [Yes]

   Justification: The research conforms with the NeurIPS Code of Ethics.

   Guidelines:

   - The answer NA means that the authors have not reviewed the NeurIPS Code of Ethics.
   - If the authors answer No, they should explain the special circumstances that require a deviation from the Code of Ethics.
   - The authors should make sure to preserve anonymity (e.g., if there is a special consideration due to laws or regulations in their jurisdiction).

10. **Broader impacts**

    Question: Does the paper discuss both potential positive societal impacts and negative societal impacts of the work performed?

    Answer: [NA]

    Justification: The proposed research does not pose any foreseeable societal risks, including those related to misinformation, bias or fairness, data privacy, or security.

    Guidelines:

    - The answer NA means that there is no societal impact of the work performed.
    - If the authors answer NA or No, they should explain why their work has no societal impact or why the paper does not address societal impact.
    - Examples of negative societal impacts include potential malicious or unintended uses (e.g., disinformation, generating fake profiles, surveillance), fairness considerations (e.g., deployment of technologies that could make decisions that unfairly impact specific groups), privacy considerations, and security considerations.

- The conference expects that many papers will be foundational research and not tied to particular applications, let alone deployments. However, if there is a direct path to any negative applications, the authors should point it out. For example, it is legitimate to point out that an improvement in the quality of generative models could be used to generate deepfakes for disinformation. On the other hand, it is not needed to point out that a generic algorithm for optimizing neural networks could enable people to train models that generate Deepfakes faster.
- The authors should consider possible harms that could arise when the technology is being used as intended and functioning correctly, harms that could arise when the technology is being used as intended but gives incorrect results, and harms following from (intentional or unintentional) misuse of the technology.
- If there are negative societal impacts, the authors could also discuss possible mitigation strategies (e.g., gated release of models, providing defenses in addition to attacks, mechanisms for monitoring misuse, mechanisms to monitor how a system learns from feedback over time, improving the efficiency and accessibility of ML).

11. **Safeguards**

    Question: Does the paper describe safeguards that have been put in place for responsible release of data or models that have a high risk for misuse (e.g., pretrained language models, image generators, or scraped datasets)?

    Answer: [NA]

    Justification: Our paper poses no such risks.

    Guidelines:

    - The answer NA means that the paper poses no such risks.
    - Released models that have a high risk for misuse or dual-use should be released with necessary safeguards to allow for controlled use of the model, for example by requiring that users adhere to usage guidelines or restrictions to access the model or implementing safety filters.
    - Datasets that have been scraped from the Internet could pose safety risks. The authors should describe how they avoided releasing unsafe images.
    - We recognize that providing effective safeguards is challenging, and many papers do not require this, but we encourage authors to take this into account and make a best faith effort.

12. **Licenses for existing assets**

    Question: Are the creators or original owners of assets (e.g., code, data, models), used in the paper, properly credited and are the license and terms of use explicitly mentioned and properly respected?

    Answer: [Yes]

    Justification: Our paper properly cite all relevant assets.

    Guidelines:

    - The answer NA means that the paper does not use existing assets.
    - The authors should cite the original paper that produced the code package or dataset.
    - The authors should state which version of the asset is used and, if possible, include a URL.
    - The name of the license (e.g., CC-BY 4.0) should be included for each asset.
    - For scraped data from a particular source (e.g., website), the copyright and terms of service of that source should be provided.
    - If assets are released, the license, copyright information, and terms of use in the package should be provided. For popular datasets, `paperswithcode.com/datasets` has curated licenses for some datasets. Their licensing guide can help determine the license of a dataset.
    - For existing datasets that are re-packaged, both the original license and the license of the derived asset (if it has changed) should be provided.

- If this information is not available online, the authors are encouraged to reach out to the asset's creators.

13. **New assets**

    Question: Are new assets introduced in the paper well documented and is the documentation provided alongside the assets?

    Answer: [NA]

    Justification: Our paper does not release new assets.

    Guidelines:

    - The answer NA means that the paper does not release new assets.
    - Researchers should communicate the details of the dataset/code/model as part of their submissions via structured templates. This includes details about training, license, limitations, etc.
    - The paper should discuss whether and how consent was obtained from people whose asset is used.
    - At submission time, remember to anonymize your assets (if applicable). You can either create an anonymized URL or include an anonymized zip file.

14. **Crowdsourcing and research with human subjects**

    Question: For crowdsourcing experiments and research with human subjects, does the paper include the full text of instructions given to participants and screenshots, if applicable, as well as details about compensation (if any)?

    Answer: [NA]

    Justification: Our paper does not involve crowdsourcing nor research with human subjects.

    Guidelines:

    - The answer NA means that the paper does not involve crowdsourcing nor research with human subjects.
    - Including this information in the supplemental material is fine, but if the main contribution of the paper involves human subjects, then as much detail as possible should be included in the main paper.
    - According to the NeurIPS Code of Ethics, workers involved in data collection, curation, or other labor should be paid at least the minimum wage in the country of the data collector.

15. **Institutional review board (IRB) approvals or equivalent for research with human subjects**

    Question: Does the paper describe potential risks incurred by study participants, whether such risks were disclosed to the subjects, and whether Institutional Review Board (IRB) approvals (or an equivalent approval/review based on the requirements of your country or institution) were obtained?

    Answer: [NA]

    Justification: Our paper does not involve crowdsourcing nor research with human subjects.

    Guidelines:

    - The answer NA means that the paper does not involve crowdsourcing nor research with human subjects.
    - Depending on the country in which research is conducted, IRB approval (or equivalent) may be required for any human subjects research. If you obtained IRB approval, you should clearly state this in the paper.
    - We recognize that the procedures for this may vary significantly between institutions and locations, and we expect authors to adhere to the NeurIPS Code of Ethics and the guidelines for their institution.
    - For initial submissions, do not include any information that would break anonymity (if applicable), such as the institution conducting the review.

16. **Declaration of LLM usage**

Question: Does the paper describe the usage of LLMs if it is an important, original, or non-standard component of the core methods in this research? Note that if the LLM is used only for writing, editing, or formatting purposes and does not impact the core methodology, scientific rigorousness, or originality of the research, declaration is not required.

Answer: [Yes]

Justification: Our paper describes the usage of LLMs to do drug design.

Guidelines:

- The answer NA means that the core method development in this research does not involve LLMs as any important, original, or non-standard components.
- Please refer to our LLM policy (`https://neurips.cc/Conferences/2025/LLM`) for what should or should not be described.